This letter lists the main changes we have made in the manuscript to take into account the two reviews and provides a list of all relevant changes made in the manuscript.

More details of our reply to the reviewer comments are given on the BGD site.

In the initial submitted manuscript the results were presented following only two sections: Trends in region C-D-E and Trends in region B. Following the suggestions from the reviewers and to clarify the results and discussion, the sections of the manuscript have been revised and rearranged as follows:

1 Introduction

2 Material and Methods

2.1 Data collection and measurements

- 2.2 Calculations of the carbonate system parameters and contributions
- 2.3 Data selection: regions and seasons

3 Results

- 3.1 Seasonal cycle
- 3.2 Long-term trend and anthropogenic CO₂
- 3.3 Winter trends at different periods
- 3.4 Summer trends at different periods

4 Discussion

5 Conclusion and perspectives

1. Data

A reviewer seems disappointed with the new data and results that would offer "practically nothing new" with respect to previous work. In the present study, we added ten years of data (2008-2017) which offer new and complementary results. The paper by Reverdin et al. (ESSD, 2018b) aimed at describing in detail the methods, accuracy and data for the full period 1993-2017 (with some data revisited and corrected): Reverdin et al. (2018b) did not investigate internal processes or external forcing resulting in the observed temporal changes of the properties (SST, SSS, nutrients, TA and DIC, δ^{18} O and δ^{13} C). The present paper is aimed at better understanding the changes in the carbonate system over the whole period (1993-2017) and for different regions and periods, including summertime (not evaluated in previous work, Metzl et al., 2010) as well as for pH and Omega trends. This is more clearly stated in the revision. Note that the new data for 2008-2017 were obtained when NAO and AMO variability were large and this is now discussed in more details as recommended by both reviewers. We also think that although challenging, it is important to start evaluating and, when possible, explain the trends observed during the summer season.

Seasonal cycle and the selection of periods:

A reviewer questioned whether the seasonal cycle should be presented in the submitted manuscript. We agree with the reviewer that the seasonal cycle is not a prime objective of the study. However, for the trend analysis, as we don't always have observations in February (winter) or July (summer), the climatological seasonal cycle is used to group data of different months (such as JFM and JJA) in order to best estimate the trends and drivers for different seasons. We thus briefly introduce and describe the seasonality in section 3.1. In years when observations were not collected in July or February (the months selected to represent summer and winter trend), we use data collected in the previous or next

month by correcting for the climatological seasonal change between successive months. As suggested by the reviewers we verified that this can be done with the more regularly-observed SST and SSS data, based on the binned monthly products constructed by Reverdin et al. (2018a). We also used this new binned-product to select the three periods investigated in more detail (1993-1997, 2001-2007 and 2008-2017), in connection with NAO and AMO indices and added a new figure to present both SST, SSS anomalies and NAO/AMO indices (new Fig. 3).

2. Method

Are Olsen suggested to explicitly take into account salinity changes in the pCO₂ driver decomposition. In the revised manuscript, we considered a new equation of attribution for SST, SSS, DIC and TA effects on pH, fCO₂ and Ω . We now consider separately the effect of salinity and sDIC, sTA (DIC and TA normalized) as recommended. Therefore, we have added trend estimates for sDIC and sTA in Table 2, present sDIC and sTA in Figure 4, and added the effects of sDIC and sTA in Figure 5 (as drivers).

Also, as mentioned by Are Olsen, uncertainties were not properly dealt with. To correct this error, we used the most recent CO2SYS software provided by James Orr (as this includes error propagation), and propagated the errors in fCO_2 (and others terms) for the trends using a Monte Carlo method. For that, we used the measurement errors of each input parameter (SST, SSS, DIC, TA, nutrients).

3. Results and discussion (processes, NAO, AMO):

A reviewer found that the relationship between the drivers and the main processes occurring in North Subpolar gyre was unfortunately very poorly developed partly because "the authors seem to be unaware of key articles that have demonstrated the main patterns of variation linked to the NAO (Thomas et al. 2008, Keller et al. 2012, Schuster et al. 2013 and Pérez et al. 2013)". In terms of acidification rates, the article by Garcia-Ibañez et al. (2016) was also ignored.

As recommended by the two reviewers we have extended the discussion including the link (or the absence of a link) with NAO and AMO and added new references as suggested, either based on observations or models. Note that recent publications, not available when we submitted our manuscript, have also been added to better discuss and compare our results (e.g. Lebehot et al., 2019; Omar et al., 2019; Holliday et al., 2019; Fröb et al 2019)

With respect to the processes, we discussed in more detail the different drivers for each period and when possible referred to observed change in productivity (for summer) or convection/mixing (for winter). In addition, as we observed significant changes in the TA trends, we discussed this result in more details in the revised version and suggest a possible link with calcification (although not yet quantify but might be relevant for further studies).

4. Anthropogenic versus non-anthropogenic signal issue

The reviewers asked to better separate the anthropogenic and non-anthropogenic signals. The first version of this paper did not separate anthropogenic and natural signals of CO_2 . In the new version, we have estimated and compared the anthropogenic signal of DIC in the NASPG based on different data and methods (Glodap-V2, Gruber et al., 2019). This is now described and discussed in Section 3.2 for the long-term trend analysis (1993-2017) as well as in the Discussion, section 4. We also evaluate and

show the impact of both anthropogenic (C-ant) and natural (DIC-nat) signals to explain the drivers and a better identification of the period when the natural variability dominates. A new figure (Fig. 6) is now added to show these effects for long-term, each period and each region.

5. Figures and Tables

In the revised manuscript we have prepared:

A new single figure (Fig. 1) as recommended, which summarized the SURATLANT cruises track and boxes considered for the trend analysis.

In Figure 2 we have added the atmospheric fCO₂ to highlight the ocean CO₂ source/sink seasonality.

A new Figure 3 presents the SST and SSS anomalies for winter along the SURATLANT track (based on binned products constructed by Reverdin et al. (2018a). This also shows the 3 different periods selected for the trend analysis. Figure 3c also includes the NAO and AMO index during this period and used in the description of the results and in the discussion section.

In Figure 4 we added a figure of the air-sea fCO_2 differences (Fig. 4h) as suggested by Are Olsen to illustrate the change of the ocean CO_2 sink that is discussed in more detail in the revised manuscript (including comparison with other recent results, Lebehot et al., 2019; Denvil-Sommer et al., 2019 among others).

In Figure 4 we also added normalized DIC and TA (Fig. 4d, f).

In Figure 5 we now add the effects of sDIC and sTA for each period and region.

A new Figure 6 presents the decomposition of the trends for pH according to the effect of the changes in total, natural and anthropogenic DIC.

Table 2: All values have been recalculated according to the error analysis and selection of data (e.g. for summer 2007-2017 the data in July 2013 are not taken into account; this is explained in the manuscript).

Table 2: Trends for sDIC and sTA have been added.

Ocean carbonate system variability in the North Atlantic Subpolar surface water (1993-2017)

Coraline Leseurre¹, Claire Lo Monaco¹, Gilles Reverdin¹, Nicolas Metzl¹, Jonathan Fin¹, Solveig Olafsdottir² and Virginie Racapé³

⁵ ¹Laboratoire d'Océanographie et du Climat-: Expérimentation et Approches Numériques (LOCEAN-IPSL), Sorbonne Université-CNRS-IRD-MNHN, Paris, 75005, France
 ² Marine and Freshwater Research Institute (MFRI), Reykjavik, Iceland
 ³Laboratoire d'Océanographie Physique et Spatiale (LOPS), CNRS-IFREMER-IRD-UBO, Plouzané, 29280, France

10 Correspondence to: Coraline Leseurre (coraline.leseurre1@gmail.com)(coraline.leseurre@locean-ipsl.upmc.fr)

Abstract. The North Atlantic is one of the major <u>ocean</u> sinks for <u>natural and anthropogenic atmospheric CO₂. Given the variability of the</u> circulation, convective processes or warming/cooling recognized in the high latitudes in this region, a better understanding of the CO₂ sink temporal variability and associated acidification needs a close inspection of seasonal, interannual to multidecadal observations. In this study, we investigate the evolution of CO₂ uptake and ocean acidification in the North Atlantic Subpolar Gyre (50°N-64°N) using repeated observations

- 15 collected over the last three decades in the framework of the long-term monitoring program SURATLANT (SURveillance de l'ATLANTique). Over the full period (1993-2017) the trend of fugacity of CO_2 (f CO_2) in surface waters (+1.70 µatm yr⁻¹) is slightly less than the atmospheric rate (+1.96 µatm yr⁻¹) and the pH decrease (-0.0017 yr⁻¹). This is mainly due to dissolved inorganic carbon (DIC) increase associated with the anthropogenic signal. However, over shorter periods (4-10 years) and depending on the season we detect significant variability investigated in more detail in this study. Data obtained between 1993 and 1997 suggest an important reduction in the capacity of the ocean to absorb CO_2 from
- 20 the atmosphere during summer, due to a rapid increase in the fugacity of CO_2 (fCO₂) in surface waters (5 (7) times faster than the increase in the atmosphere). This was associated with a rapid decrease in surface pH (of the order of -0.014/016 yr⁻¹) and was mainly driven by a significant warming and <u>an</u> increase in DIC. Similar <u>fCO₂</u> trends are observed between 2001 and 2007 during both summer and winter with a mean decrease of pH between 0.006/yr and -0.013/yr. These rapid but, without significant warming detected, these trends are mainly explained by a significant warming of surface waters, an increase in DIC and a decrease in alkalinity during summer and an increase in DIC during winter. This also leads
- 25 <u>to a pH decrease but with contrasting trends depending on the region and season (between -0.006 yr⁻¹ and -0.013 yr⁻¹).</u> On the contraryopposite, data obtained during the last decade (2008-2017) <u>in summer</u> show a stagnation of surface fCO_2 (increasing the ocean sink for CO_2) and pH. These recent trends are explained by the cooling of surface waters, a small decrease of total and an increase in alkalinity and the near stagnation of dissolved inorganic carbon., leading to a strong decrease of surface fCO_2 (between -4.4 and -2.3 µatm yr⁻¹; i.e. the ocean CO_2 sink increases). Surprisingly, during summer, pH increases up to +0.0052 yr⁻¹ in the southern subpolar gyre. Overall our results show that, in addition to the
- 30 <u>accumulation of anthropogenic CO₂, the temporal changes of</u> the uptake of CO₂ and ocean acidification in the North Atlantic Subpolar Gyre is substantially impacted by multi-decadalpresent significant pluriannual variability, in addition to the accumulation of anthropogenic CO₂. As a consequence, the not clearly directly associated with the North Atlantic Oscillation (NAO). With such variability it is uncertain to predict the near-future evolution of air-sea CO₂ fluxes, pH and the saturation state of surface waters with regards to aragonite and calcite remain highly uncertain-pH in this region. Thus it is highly recommended to maintain long-term observations to monitor these properties in the next decade.

35 1 Introduction

Observations have shown an increase by more than 40% in atmospheric carbon dioxide (CO_2) since the industrial revolution, resulting in the strengthening of the greenhouse effect (IPCC, 2013 – Hartmann et al., 2013). Despite increasing efforts at the international level to tackle climate change, the last carbon report published by Le Quéré et al. (2018) shows that CO_2 emissions reached 11.3 ± 0.9 GtC in 2017, mainly due to the

burning of fossil fuels (9.9 \pm 0.5 GtC in 2017, three time higher than in 1960). The ocean plays an important role in climate regulation by absorbing between one quarter and one third of this anthropogenic carbon (Le Quéré et al., 2018; Gruber et al., 2019). The North Atlantic is known as one of the main anthropogenic CO₂ sinks (Sabine et al., 2004; Khatiwala et al., 2013): this region (north of 50°N), covering 5% of the global surface ocean, is responsible for 20% of the oceanic uptake of anthropogenic CO₂ (Khatiwala et al., 2013), with a mean annual air sea

5 CO₂ flux estimated at 0.27 PgC/yr (Takahashi et al., 2009). The uptake of CO₂ in the North Atlantic is mainly due to extensive biological activity during summer and considerable heat loss during winter. However, repeated observations have shown important variations in this natural sink for anthropogenic CO₂ in response to climate variability and climate change (Corbière et al., 2007; Metzl et al., 2010; McKinley et al., 2011; Landschützer et al., 2013).

In addition to climate change, CO₂ emissions are responsible for ocean acidification, a phenomenon known as the other CO₂ problem (Doney et

- 10 al., 2009). Indeed, the accumulation of anthropogenic CO₂-in the ocean has led to a decrease in pH in surface waters by 0.1 unit since the industrial revolution (IPCC, 2013 Hartmann et al., 2013). Due to the potential threat on marine life, the decrease in pH is recognized as a true indicator of global change, similarly as warming and sea level rise (World Meteorological Organization, 2018). The urgent need for documenting and understanding changes in oceanic pH and its impact on marine life has motivated more studies in recent years. Among them, the data syntheses from Lauvset et al. (2015) and Bates et al. (2014) indicated that pH is decreasing in most of the surface ocean as a result of the increase
- 15 in oceanic CO₂. In the North Atlantic they reported a decrease ranging between 0.001/yr and 0.003/yr. These estimates were obtained by combining all available data either at fixed monitoring stations in the Iceland Sea, Irminger Sea and offshore Bermuda over the period 1983-2014 (Bates et al., 2014), or in the North Atlantic Subpolar Seasonally Stratified biome over the period 1991-2011 (Lauvset et al., 2015). Here, we use repeated observations collected between Iceland and Newfoundland to investigate further the change in surface pH by evaluating separately summer and winter data, and by taking into account changes in the North Atlantic Subpolar Gyre (NASPG) circulation and water
- 20 masses (Chafik et al., 2014; Desbruyères et al., 2015; Nigam et al., 2018). This study, based on Total Alkalinity (TA) / Dissolved Inorganic Carbon (DIC) pair observations, allows to evaluate their contribution; while most studies are based on observations of partial pressure of CO₂ (pCO2) and TA/Salinity (Lauvset and Gruber, 2014). The aim of this study is to document the evolution of the CO₂ system parameters in recent years (up to 2017) and to evaluate the drivers for the evolution of surface pH for winter and summer. In this respect, it extends previous analyzes based on SURATLANT observations collected during winter between 1993 and 2008 (Corbière et al., 2007; Metzl et al., 2010).

25 2 Study area

The ocean plays an important role in climate regulation by absorbing between one quarter and one third of anthropogenic carbon dioxide (CO_2) emitted to the atmosphere (Le Quéré et al., 2018; Gruber et al., 2019). The North Atlantic (NA) is one of the strongest ocean sinks for natural (Takahashi et al., 2009) and anthropogenic atmospheric CO_2 (Khatiwala et al., 2013; Sabine et al., 2004; Perez et al, 2008). Although many observational studies were conducted in the NA to evaluate how the CO_2 sink varies from seasonal to multi-decadal scales and modeling studies

- 30 attempted to reproduce the observed changes, there are still open questions regarding the processes that control the contemporary CO₂ sink variability in this region (e.g. Schuster et al., 2013, for a synthesis). The uptake of CO₂ in the NA is mainly due to extensive biological activity during spring-summer and considerable heat loss during winter, both processes being subject to significant spatio-temporal variability related to climate mode such as the North Atlantic Oscillation (NAO) and the Atlantic Multidecadal Variability (AMV), also called Atlantic Multidecadal Oscillation (AMO). The recent decades have indeed witnessed large variations of the NAO index (Hurrell index, 2013) which displayed strong
- 35 positive indices in the early 1990s, then from 1996 to the early 2000 tended to be positive, and has then been more neutral, albeit with extreme anomalies, such as the negative 2010 event, until again witnessing large positive anomalies in the mid 2010s. The NA has also being at the core of large decadal to multi-decadal variability of the AMV with a positive peak by the mid 2000 and a decrease since then (Robson et al., 2018). In the North Atlantic Subpolar Gyre (NASPG, around 50-60°N) where the oceanic CO₂ sink is particularly strong (e.g. Watson et al., 2009), recent years in the mid-2010s have also witnessed particularly large negative surface temperature anomalies (Josey et al., 2018) and an extreme
- 40 freshening (Holliday et al., 2019). Associated changes in the ocean circulation and water masses in the NASPG are for example presented in

Chafik et al. (2014, 2019); Desbruyères et al. (2015); Nigam et al. (2018). These physical processes linked to NAO and/or AMV directly impact the sea surface fCO_2 and air-sea CO_2 fluxes through warming/cooling or deeper convection as this has been observed in the NASPG for specific periods (Corbière et al., 2007; Fröb et al., 2019). However, a direct link of the CO_2 uptake variability with the NAO depends on the period investigated and this is not always clearly revealed from observations (Metzl et al., 2010; Schuster et al., 2013).

5

10

Ocean models and Earth System Models (ESM) can help to understand the link between NAO and biogeochemical cycles, but results from models in the NA are still controversial (Thomas et al., 2008; Ullman et al., 2009; Keller et al., 2012; Tjiputra et al., 2012). Keller et al. (2012) investigated simulations from 6 ESMs and found that the inter-annual variability of the CO_2 sink in the North Atlantic is the largest in the subpolar gyre. They also conclude that for winter (i.e. not the productive season) on-site entrainment in the NASPG (mixing and upwelling) is the main driver of carbon sink variability as opposed to advection (Thomas et al., 2008), but the magnitude and responses of the carbon uptake

to the NAO significantly differ between the ESM models (Keller et al., 2012). Thomas et al. (2008) suggest that negative or neutral NAO conditions result in a substantial decline of the CO₂ uptake for the years 1997-2004 along the North Atlantic Current region (NAC) and in the eastern subpolar gyre. On the opposite Ullman et al. (2009) conclude that the CO₂ uptake increased over 1992–2006. During the transition of NAO (from positive to neutral), their model simulates a decline of the convection and vertical DIC supply to the surface in the subpolar region,

15 counteracting the increase of pCO_2 due to warming. This leads to a relatively small pCO_2 increase compared with the atmospheric CO_2 trend and an increasing CO_2 sink, while observations in 1993-2003 suggest a reduced CO_2 sink in the NASPG after the NAO shift in the mid-90s (Corbière et al., 2007).

For longer timescales, two decades or more, observations in the NASPG show a gradual fCO₂ increase slightly smaller or indistinguishable from
 trends in atmospheric CO₂ and that the long-term oceanic fCO₂ trend is not correlated with NAO (Takahashi et al., 2009; McKinley et al., 2011; Fay and McKinley, 2013). On decadal scale the link between AMO and fCO₂ variability in the NASPG appears more robust (Breeden and McKinley, 2016; Landschützer et al., 2019). When AMO enters in a positive phase these studies indicate a reduction of DIC in the NASPG due to reduced mixing, a process that dominates the effect of warming on fCO₂ (Breeden and McKinley, 2016). Consequently since the mid-1990s the fCO₂ long-term trend lagged the one in the atmosphere and the CO₂ uptake is increasing in this region. Such signal is not captured by current

25 ESM CMIP5 models (Tjiputra et al., 2014; Lebehot et al., 2019) likely due to inadequate representation of biogeochemical cycles (here DIC and/or TA). This leads to uncertainties regarding the evolution of the oceanic CO₂ uptake in the North Atlantic in the future (Lebehot et al., 2019). A better knowledge of DIC and TA trends (not only fCO₂) is needed to correct and validate biogeochemical representation in ESM models.

- 30 The response of the marine biological processes to NAO and AMO are much less studied than their physical counterpart. However and somehow, as for fCO₂, the biology link seems also better identified with AMO than with NAO. Based on the biomass variability detected from SeaWIFS over 1998-2007 in the North Atlantic and supported by biogeochemical simulations McKinley et al. (2018) conclude that "nowhere is the NAO correlated with biomass variability". The same is true, i.e. no correlation with NAO, when analyzing long-term in-situ observations of marine species in the NA since the 60s (Beaugrand et al., 2013; Rivero-Calle et al., 2015). However these authors detect significant increase of calcifying
- 35 species (coccolithophores, foraminifera) associated to the warming in the NA since the mid-90s and correlated with AMO. This increase in calcification would impact the DIC and TA concentrations in summer and thus the fCO_2 trend and carbon uptake in the NA. On the other hand, this also suggests that these phytoplanktonic groups are not yet altered by acidification, a phenomenon known as the other CO_2 problem (Doney et al., 2009). Indeed, the accumulation of anthropogenic CO_2 in the ocean has led to a decrease in pH in surface waters by 0.1 unit since the industrial revolution (IPCC, 2013 Hartmann et al., 2013). It is projected that surface pH would be reduced by 0.2 to 0.4 unit by the end of the
- 40 century depending on the anthropogenic emission scenario (Orr et al., 2005; Doney et al., 2014; Jiang et al., 2019). This would be associated with a dramatic shoaling of the aragonite saturation horizon at high latitudes, from 2000 m at present up to 100 m by 2100 in the North Atlantic (north of 50°N) due to deep penetration of high concentrations of anthropogenic CO₂. Such fast lysocline shoaling based on a simulation (Orr

et al., 2005) is started to be observed in this region (e.g. Vázquez-Rodríguez et al., 2012). Due to the potential threat on marine life, the decrease in pH is now recognized as a true indicator of global change, similarly to warming and sea level rise (World Meteorological Organization, 2018). The urgent need to document and understand changes in oceanic pH and its impact on marine life has motivated more studies in recent years. Among them, the data syntheses from Lauvset et al. (2015) and Bates et al. (2014) indicated that pH is decreasing in most of the surface ocean

5 as a result of the increase in oceanic CO₂. In the North Atlantic they reported a decrease of pH ranging between -0.001 yr⁻¹ in the subtropical region and -0.0026 yr⁻¹ in the Irminger Sea. These results have been confirmed at a regional scale. Based on 12 cruises conducted in summer between 1991 and 2015 in the Irminger and Iceland basins, García-Ibáñez et al. (2016) identified a pH decrease in all water masses, with largest change in surface and intermediate waters of between -0.0016 to -0.0018 unit yr⁻¹ and conclude that it is mainly due to anthropogenic CO₂ and modulated by change in alkalinity. Recently Omar et al. (2019) analyzed regular surface observations during 2004-2015 in the North Sea; when

selecting winter data in the North Atlantic surface waters they found significant long-term trends of fCO₂ and pH of +2.4 µatm yr⁻¹ and -0.0024 10 yr⁻¹, consistent with results obtained in the subpolar North Atlantic (Bates et al., 2014; Lauvset and Gruber, 2014). A driver analysis indicates that fCO₂ and pH trends are almost entirely explained by increasing DIC due to anthropogenic CO₂ uptake (Omar et al., 2019).

As anthropogenic CO₂ accumulates each year in the surface and interior ocean with direct impact on both air-sea CO₂ exchange and pH, it is important to conduct and maintain regular observations to follow the evolution of the ocean carbonate system properties and interpret how they 15 vary from inter-annual to multi-decadal scales in relation with physical and biological changes. The aim of this study is to document the recent evolution of the surface CO₂ system parameters in the NASPG and to evaluate the drivers for the evolution of surface fCO₂ and pH for winter and summer. We mostly use Total Alkalinity (TA) and Dissolved Inorganic Carbon (DIC) discrete observations, while other studies are based on observations of partial pressure of CO₂ (pCO2) and TA/Salinity relations (Lauvset and Gruber, 2014; Lauvset et al., 2015). The observations were collected in 1993-2017 between Iceland and Newfoundland and this extends previous analyses based on winter SURATLANT observations 20 in 1993-2008 to both summer and winter time (Corbière et al., 2007; Metzl et al., 2010).

The NASPG as defined here extends from the east coast of Canada (65°W) to the west coast of IrelandNorthern Europe (5°W) mostly north of 5045°N- (Figure 1). It consists mostly of the Labrador, Irminger and Iceland basins, and the Rockall Plateau and Trough. The NASPG is a region

- of mixing between subtropical, subpolar and polar surface waters. The inflow of these surface waters is dominated by three surface currents: 25 The North Atlantic Current (NAC), also known in this sector as the North Atlantic Drift, mostly of tropical origin, the East Greenland Current (EGC) and the Labrador Current (LC) which are the conducts tothat bring waters from further north and the Arctic (Fig. 1a b1). The North Atlantic Drift delimits the NASPG in the south and transports warm (8°C to 15°C) and salty (35 to 36) tropical surface waters to the north. These waters are then cooled as they circulate in the NASPG due to a loss of heat to the atmosphere, while they become less salty due to excess local
- 30 precipitation and freshwater inputs from the Arctic and the ice sheet. The East Greenland Current (EGC) and Labrador Current (LC) are the western branches of the NASPG and carry cold (<4°C) and low saltfresh (<34.6) waters of polar origin. The study area is mostly in the central part of the NASPG between Iceland and Newfoundland.

Hydrological and biogeochemical properties in the NASPG are impacted by very large variations associated with Atlantic Multi decadal Variability (AMV), witch result from atmospheric conditions such as the North Atlantic Oscillation (NAO) (Josey et al., 2011; Reverdin, 2010; Robson et al., 2016).

35

40

32 Material and Methods

<u>32</u>.1 Data collection and measurements

This study is based on observations collected in the framework of the long-term monitoring program SURATLANT (SURveillance de l'ATLANTique) initiated in 1993. The main objective of this program is to monitor hydrological and biogeochemical properties in surface waters of the NASPG, notably Sea Surface Salinity (SSS) to improve the understanding of the role of salinity on the variability and predictability of climate as well as the water cycle (Reverdin et al., 2018a). To this aim, two to four cruises per year are conducted between Reykjavik (Island) and Newfoundland (Canada) aboard(Reverdin et al., 2018a; Holliday et al., 2019). To this end, two to four cruises per year are conducted between Reykjavik (Iceland) and Newfoundland (Canada) on board merchant ships. Seawater samples are collected every three to four hours from a pumping system (at approximately 5m deep) in order to measure salinity, as well as Total Alkalinity (TA, alkalinity (measured since 2001), Dissolved Inorganic Carbon (DIC), silicate, nitrate and phosphate concentrations.

- Underway measurements of Sea Surface Temperature (SST) are obtained using a Seabird Thermosalinograph, with a precision of 0.10°C. SSS values in this paper are from sample measurements of conductivity using a Guidline AUTOSAL salinometer done since 1997 at the Marine and Freshwater Research Institute (MFRI) in Reykjavik (the associated error is estimated at 0.005). For TA and DIC, the 500 ml glass bottles are rinsed three times before introducing seawater (avoiding introducing air bubbles) with an overflow in order to remove the water in contact with
- 10 air during filling. The samples are then poisoned with mercuric chloride and stored in a cool, dark place. Since 2001, these samples are measured within three months of collection at the SNAPO-CO₂ (Service National d'Analyse des Paramètres Océaniques du CO₂) located at the Laboratory LOCEAN in Paris. The accuracy is of the order of 3 μmol/kg for both DIC and TA based on CRMs analysis and occasional intercomparisons as explained by Reverdin et al. (2018b). Samples for the analysis of nutrients concentrations are frozen just after sampling. Spring or summer samples are filtered before analysis. The measurement is carried out by the MFRI team in Reykjavik according to the standard colorimetric
- 15 method described by Olafsson et al. (2010) with an accuracy of 0.2 μmol/l for nitrate and silicate and 0.03 μmol/l for phosphate. Detail of the sampling and analyses for all properties are provided in Reverdin et al. (2018b). The SURATLANT dataset is freely available and is accessible at

Underway measurements of Sea Surface Temperature (SST) are obtained using a Seabird Thermosalinograph, with a precision of $\pm 0.1^{\circ}$ C. SSS values in this paper are from sample measurements of conductivity using a Guidline AUTOSAL salinometer done since 1997 at the Marine and

- 20 <u>Freshwater Research Institute (MFRI) in Reykjavik (the associated error is estimated at ± 0.005). For TA and DIC, the 500 ml glass bottles are rinsed three times before introducing seawater (avoiding introducing air bubbles) with an overflow in order to remove the water in contact with air during filling. The samples are then poisoned with mercuric chloride and stored in a cool, dark place. Since 2001, these samples are measured within three months of collection at the SNAPO-CO₂ (Service National d'Analyse des Paramètres Océaniques du CO₂) located at the Laboratory LOCEAN in Paris. The accuracy is of the order of $\pm 3 \mu$ mol kg⁻¹ for both DIC and TA based on CRMs analysis and occasional intercomparisons</u>
- 25 as explained by Reverdin et al. (2018b). Samples for the analysis of nutrients concentrations are frozen just after sampling. Spring or summer samples are filtered before analysis. The measurement is carried out by the MFRI team in Reykjavik according to the standard colorimetric method described by Ólafsson et al. (2010) with an accuracy of $\pm 0.2 \mu mol l^{-1}$ for nitrate and silicate and $\pm 0.03 \mu mol l^{-1}$ for phosphate. Details of the sampling and analyses for all properties are provided in Reverdin et al. (2018b). The SURATLANT dataset is freely available and is accessible at http://www.seanoe.org/data/00434/54517/-
- 30 <u>3.</u> In the SURATALANT data file, each sample and data is associated with a quality flag (based on WOCE flag criteria, i.e. same as used in GLODAP data-base, Olsen et al. (2016). In this study we use only data qualified with flag 2 (acceptable data).

2.2 Calculations of the carbonate system parameters and contributions

5

Carbonate system parameters such as pH, the fugacity of CO₂ (fCO₂) and the saturation states for the calcium carbonate minerals calcite (Ω_{Ca}) and aragonite (Ω_{At}) are calculated using measurements of SST, SSS, TA, DIC, silicate and phosphate. For the latter two, we used climatological
 values derived from the SURATLANT data over the period 1993-2017 because interannual variability does not have a significant impact on the carbonate system parameters calculations (and because sometimes nutrients measurements were not performed). The calculation program used is CO2SYS developed by Lewis et al. (1998) and available for calculations in MS Excel (Pierrot, et al., 2006). The constants of the thermodynamic equilibrium of CO₂ in seawater used are: K1 (for the dissociation of carbonic acid) and K2 (for the bicarbonate ion) defined by Mehrbach et al. (1973), refitted by Dickson and Millero (1987). The total boron value is calculated according to Uppström (1974) and the KHSO₄

40 dissociation constant is from Dickson (1990). The adopted pH scale is total scale.

When TA was not measured (notably before 2001), it was calculated from salinity data. The relationship between sea surface alkalinity and salinity (Eq. 1) was determined by Reverdin et al. (2018) based on all the reported SURATLANT data over the period 2001-2016. This equation was obtained for samples collected north of 50°S with SSS > 34.

Carbonate system parameters such as pH, the fugacity of CO_2 (fCO₂) and the saturation states for the calcium carbonate minerals calcite (Ω_{Ca})

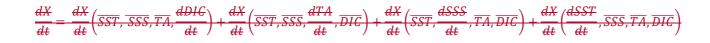
- 5 and aragonite (Ω_{Ar}) are calculated using SST, SSS, TA, DIC, silicate and phosphate data described by Reverdin et al. (2018b). For the latter two, we used monthly climatological values derived from the SURATLANT data over the period 1993-2017 because nutrients inter-annual variability does not have a significant impact on the carbonate system parameters calculations (and because nutrients were missing for some cruises). The calculation program used is CO2SYS originally developed by Lewis et al. (1998) available in MATLAB version (van Heuven et al., 2011) that now includes error propagation (Orr et al., 2018). The constants of the thermodynamic equilibrium of CO₂ in seawater used are: K₁ (for the
- 10 dissociation of carbonic acid) and K_2 (for the bicarbonate ion) defined by Mehrbach et al. (1973), refitted by Dickson and Millero (1987). The total boron value is calculated according to Uppström (1974) and the KHSO₄ dissociation constant is from Dickson (1990). The adopted pH scale is total scale.

When TA was not measured (notably before 2001), it was calculated from salinity data. The correlation between sea surface alkalinity and
 salinity in the open ocean can be described with an empirical linear relationship (Millero et al., 1998; Friis et al., 2003). For the NASPG, the original TA/SSS relation used to analyze fCO₂ variability and trend in 1993-2007 (e.g. Corbière et al., 2007; Metzl et al., 2010; McKinley et al., 2011) was revisited by Reverdin et al. (2018b) based on SURATLANT data over the period 2001-2016 (Eq. 1). This equation was obtained for samples collected north of 50°N with SSS > 34.

 $TA = 45.5337 \times SSS + 713.58$,

(1)

- 20 Atmospheric fCO₂ values for the period 1993 2017 were calculated from the molar fraction (xCO₂) data at Mace Head provided by the Cooperative Global Atmospheric Data Integration Project (Dlugokencky et al., 2018). The data are available at http://www.esrl.noaa.gov/gmd/dv/iadv/). xCO₂ data were converted to fCO₂ at 100% humidity following Weiss and Price (1980). We did not take into account the interannual variability of surface atmospheric pressure, which can result in small errors on interannual deviations of atmospheric fCO₂.
- 25 To evaluate the air-sea CO₂ difference (delta-fCO₂) for each sample we used atmospheric fCO₂ values for the period 1993-2017 calculated from the molar fraction (xCO₂) data at Mace Head provided by the Cooperative Global Atmospheric Data Integration Project (Dlugokencky et al., 2018). The xCO₂ data are available at http://www.esrl.noaa.gov/gmd/dv/iadv/ last access 06/03/2019). xCO₂ data were converted to fCO₂ at 100% humidity following Weiss and Price (1980), with standard atmospheric pressure.
- The trends in sea surface pH, fCO₂, $\Omega_{Ca^{-}}$ and $\Omega_{Ar}\Omega$ are driven by changes in SST, SSS, TA and DIC. These contributions are For DIC, this includes anthropogenic CO₂ concentration (Cant) and the DIC natural component (DIC-nat = DIC-Cant). The contribution of each term for a specific period and season is evaluated by allowing a change in only one parameter according to their observed trend, while setting the other parameters to their climatological <u>seasonal</u> values (Eq. 2). The <u>uncertainty of the</u> contributions <u>uncertainty</u>-was evaluated by performing 2001000 random perturbations within the range of the standard deviation of the observed trends in SST, SSS, TA and DIC. The same method was applied when separating the effect of DIC-nat and anthropogenic CO₂ (Cant).
- 35



$$\frac{dX}{dt} = \frac{\partial X}{\partial SST} \frac{dSST}{dt} + \frac{\partial X}{\partial SSS} \frac{dSSS}{dt} + \frac{\partial X}{\partial DIC} \left(\frac{\overline{SDIC}}{SSS_0} \frac{dSSS}{dt} + \frac{\overline{SSS}}{SSS_0} \frac{dSDIC}{dt} \right) + \frac{\partial X}{\partial TA} \left(\frac{\overline{STA}}{SSS_0} \frac{dSSS}{dt} + \frac{\overline{SSS}}{SSS_0} \frac{dSTA}{dt} \right)$$

Here, $\frac{dX}{dt}$ correspond to the trends in pH, fCO₂, Ω_{Ca} and Ω_{Ar} over a given period; and $\overline{SST}, \overline{SSS}, \overline{TA}, \overline{DIC}$ correspond to their climatological values calculated over the same period.

(2)

5 3

Here, X corresponds to pH, fCO₂, and Ω . SSS₀ is the reference salinity, which is set to 35 (Normal Standard Seawater, Millero et al., 2008) and very close to the mean salinity observed in the NASPG (SSS = 34.84). sDIC and sTA were computed by normalizing DIC and TA to a salinity of 35 and assuming a nonzero freshwater end-member DIC and TA concentration (Friis et al., 2003; Reverdin et al., 2018b). The trends (dX/dt) were estimated for each season, each boxes and periods; and \overline{SST} , \overline{SSS} , \overline{TA} , \overline{DIC} correspond to their climatological values calculated over the

10 <u>same period.</u>

2.3 Data selection : regions and seasons

The sampled region was separated into five 4° latitude boxes, according to Reverdin et al. (2018) from 46°N to 64°N (Fig. 2). The southern box (box A: 46°N 50°N) covers the shelf and continental margin of North America and is excluded from this study because of insufficient sampling and large interannual variations due to fresh waters inputs from land and the Arctic. Box B (50°N 54°N) incorporates only samples where SSS

15 is between 34 and 35 (to avoid including continental shelf or NAC waters). For boxes C (54°N 58°N), D (58°N 62°N) and E (62°N 64°N) we used all available data.

Trends during summer (June to August) and winter The sampled region was separated into five 4° latitude boxes, from 46°N to 64°N (Fig. 1) according to Reverdin et al. (2018b). The southern box (box A: 46°N-50°N) covers the shelf and continental margin of North America and is excluded in the present long-term trend analysis because of insufficient sampling and large inter-annual variations due to fresh waters inputs

- 20 from continental runoff. Box B (50°N-54°N) incorporates only samples where SSS is between 34 and 35 (to avoid including continental shelf or NAC waters). Thus, whereas over 470 samples with DIC data are found in Box-B for 1993-2017, only 399 data in the salinity range 34-35 are considered (we excluded 38 data for S<34 and 33 data for S>35). For boxes C (54°N-58°N), D (58°N-62°N) and E (62°N-64°N) we used all available data.
- 25 The trend analysis and contributions calculations (Eq. 2) was first performed for each box but results of trends and drivers for boxes C, D, E were found quasi identical. Therefore, we present and discuss the results by combining the data collected north of 54°N (i.e., boxes C, D and E). The trends in box B are evaluated separately because properties and their trends (SST, SSS, DIC, TA) differ significantly from the other three boxes. We separate seasons, and the trends for winter (January to March) were and summer (June to August) are analyzed separately because these are the seasons corresponding to the as they correspond to seasonal extrema in the seasonal cycle (see Sect. 3.1). In addition, they are also
- 30 the mostof surface carbonate properties (described below in Section 3.1) and these seasons were more regularly sampled periods foralong the SURATLANT surveysline (Table 1). Because the seasonal cycle shows month to month deviationsFinally, we choose February and July as a reference (for winter and summer, respectively). The. When February or July data were missing for a specific year, the data collected in January andor March (for winter) and in June andor August (for summer) were corrected using the month-to-month differences calculatedused after correcting the observed seasonal anomalies from the climatological cycle. cycles described in the next section (3.1). No attempt to reconstruct
- 35 <u>data was performed when the SURATLANT line was not sampled for at least 3 months (e.g. winter 2016 and 2017 not included in this analysis</u> and trends limited to 1993-2015 for this season).

In order to evaluate the decadal changes within a large region, we combined the data collected between 54°N and 63°N (i.e., boxes C, D and E). The trends in box B are evaluated separately because their DIC and TA values differ from the other three regions.

43 Results

43.1 Seasonal cycle

In order to increase the number of data used in our long term analysis (because data were not available each year in the reference months February and July, Table 1), we first constructed a monthly climatology for each property and each box, which was used to correct the data

- 5 collected in January, March, June and August. The mean seasonal cycles constructed from data collected over the period 1993-2017 are portrayed in Fig. 2. SST data (Fig. 2a) show an increase from south to north during winter (5.5°C to 6.8°C), which is not observed during summer (around 12°C in all boxes), while SSS data (Fig. 2b) and TA data (Fig 2.c) show a decrease from south to north, and small seasonal variations. DIC data (Fig. 2d) show much larger seasonal variability than TA, with a maximum in winter due to enhanced vertical mixing, a steep decline from April to May due to phytoplankton blooms, and a minimum at the end of summer. The mean seasonal cycles of fCO₂, pH and Ω (Fig. 2e h) show
- 10 fairly similar variations in boxes B, C, D and E. The seasonal changes in fCO₂ and pH are anticorrelated, and the seasonal variability of Ω is relatively similar to that of pH. In all boxes, the maximum in fCO₂ (minimum in pH and Ω) is observed between October and April and related to the maximum in surface DIC, despite the cooling of surface waters. The minimum in fCO₂ (maximum in pH and Ω) is observed during summer (between June and August), and is mainly explained by enhanced primary production, only slightly counterbalanced by sea surface waterace.

15 4.2 Decadal trends

Figure 3 clearly shows pluriannual trends in hydrological and biogeochemical properties of the NASPG. For this reason, and according to Metzl et al. (2010), the dataset is split into three distinct periods : 1993 1997, 2001 2007 and 2008 2017. Below, we first present the results obtained by combining the boxes C, D and E that are probably more representative of changes in the NASPG than the results in box B that are also influenced by continental inputs.

20 4.2.1 Trends in region C-D-E

Data collected between 1993 and 1997 show a large increase in surface fCO_2 -during summer, accompanied by a sharp decrease in pH and Ω (Fig. 3e h). This is mainly explained by a rapid increase in SST (Table 2, Fig. 4a, d, g, f). The trend in oceanic fCO_2 (+10.6 μ atm/yr) is approximately 5 times faster than the trend in atmospheric fCO_2 (around +2 μ atm/yr), which implies important changes in oceanic processes causing a reduction in the summer CO_2 -sink over this period. On the opposite, during winter, both hydrological and biogeochemical properties

25 are steady (Fig. 3).

Data collected during the second period (2001–2007) show a large increase in surface fCO_2 -during both summer and winter associated with a sharp decrease in pH and Ω (Fig. 3e h). The trend in oceanic fCO_2 (+11.7 μ atm/yr) is about 6 times faster than the trend in atmospheric fCO_2 , which implies a reduction in the ability of the ocean to absorb CO_2 from the atmosphere over the period 2001–2007 during both summer and winter. At the end of this period, in winter 2007, oceanic fCO_2 (more than 400 μ atm) became higher than atmospheric fCO_2 (around 380 μ atm;

30 i.e., the ocean became a source of CO₂ for the atmosphere). Since small trends are observed in SST over this period (Fig. 3a, Table 2), the rapid trends in fCO₂ and pH can be attributed to the increase in DIC and a decrease in TA.
 Despite the continuous increase in atmospheric fCO₂ over the last decade (around 2.0 µatm/yr), data collected over the period 2008–2017 show the near stagnation of surface fCO₂, pH and Ω. As a result, the air sea CO₂-disequilibrium increased, which means that the ocean was able to

absorb more CO₂ from the atmosphere than during the previous periods. In contrast to the previous periods, large interannual variations are observed during summer. Overall, SST, DIC and TA show small or not significant trends over the period 2008 2017 (Table 2).

4.2.2 Trends in region B

The trends in fCO_2 , pH and Ω observed in box B show some similarities with those in boxes C, D and E (Fig. 3), but the mechanisms may be different (Fig.4). For example, a rapid increase in fCO_2 (decrease in pH) is also observed in box B during summer over the first period (1993-

1997), but it is due to a large increase in DIC rather than warming (Table 2), and as a consequence, it is accompanied by a rapid decrease in Ω (Fig. 3g, h, Table 2). Over the second period (2001-2007), a rapid increase in fCO₂ (decrease in pH and Ω) is observed in all boxes during both summer and winter, mainly explained by an increase in DIC and/or a decrease in TA (depending on the region and season). Over the last period (2008-2017), the trends in fCO₂, pH and Ω in all boxes are smaller than during the previous periods (Table 2). This change in the behavior of

5 the NASPG appears to be more pronounced in box B during summer with a reversal of the trends (decrease in fCO₂ and increase in pH and Ω).

5 Discussion

Observations collected in the framework of the SURATLANT program show that long term surface trends in fCO_2 (+1.6 μ atm/yr) and pH (-0.0017 /yr) over the period 1993 2017 (Table 2, all boxes, summer and winter) are in the range of the "canonical" views for large scale surface ocean, generally interpreted by anthropogenic CO₂ uptake, but these trends are not steady and modulated by significant interannual to decadal

- 10 changes. Depending on the period and season, fCO₂ and pH increase or decrease due to contrasting and competing processes (Fig. 4). Our analysis confirms previous results, such as the rapid fCO₂ increase during winter over the period 2001 2007 (Metzl et al., 2010), but this signal is no longer observed over the period 2008 2017. It also highlights significant changes during summer over the period 2001 2007 not previously described. Thereafter we will first discuss the rapid trends observed during summer, then the recent trends observed during winter. Our observations show remarkable and rapid trends in surface pH and fCO₂ during summer both in 1993 1997 and 2001 2007; which result
- 15 from competition between SST, DIC and TA changes. Indeed, during the first period, variations in DIC alone (for southern box) and SST (for northern box) are responsible for these trends (Fig.4). This results in a larger coherent regional response. For example, the rapid increase of the DIC in Box B in summer 1993-1997 (+9 µmol/kg/yr) much faster than the anthropogenic signal suggests an increase in productivity at the beginning of the period compared to the end. During the second period, the effect of the TA decrease (potentially related to an advective process or an increase calcification) on fCO₂ and pH is not negligible, as well as the increase in SST and DIC. The trends in pH and fCO₂ presented here
- 20 are homogeneous spatially during summer and have similar magnitudes than the trends observed during winter. Thus, fCO₂ increased more rapidly in the ocean than in the air, suggesting that the CO₂ sink would have decreased over the period 2001 2007. This period is followed by the near stagnation of fCO₂ and pH over the last decade (2008 2017). This is concomitant with a strengthening of the winds during some winters, which likely enhanced vertical mixing (Fröb et al., 2018). Trends in hydrological properties show the same sign (summer and winter, north and south), indicating a large scale behavior. The weak trends in pH and fCO₂ over the last decade deviate from the already published long term
- 25 trends (Bates et al., 2014; Lauvset et al., 2015). This result highlights the sensitivity of trends in CO2 uptake and ocean acidification to the sampling period, which must be considered when comparing results with earlier estimates. These different results could be explained by contrasted natural or climate change induced variability in the NASPSS biome having compensating effects, whereas the increase in DIC due to the accumulation of anthropogenic CO₂ is more homogeneous in space. More regional studies are needed to check this hypothesis and to validate estimates obtained by combining data over large regions such as the North Atlantic SubPolar Seasonally Stratified (NASPSS) biome. There is also a need to further investigate the drivers of TA variability, which seem partially decoupled from surface salinity in this part of the North

Atlantic subpolar gyre.

To summarize, our observations collected over the last three decades show an abrupt change in the evolution of hydrological and biogeochemical properties in the NASPG around the year 2007. This result is consistent with the studies by Robson et al. (2012, 2016) who reported a rapid warming since the mid 1990s, followed by a cooling by approximately 0.45°C since about 2005. This change is associated with a change in the size of the gyre and increased inputs of subtropical waters from the south (Chafik et al., 2014; Desbruyères et al., 2015), as well as very large heat loss during positive Nord Atlantic Oscillation (NAO) years. Furthermore, the recent study of Landschützer et al. (2019) highlights the dominant role of the Atlantic Multi decadal Variability (AMV) which transitioned to a positive phase (i.e., warming) in the 1990's (McKinley et al., 2011), and shows a strong correspondence between AMV and thermally driven pCO₂-variations, which can be extrapolated to our study.

40 Indeed, the region investigated in this study (boxes C, D, E) is directly imprinted by NAO (at all periods, according to the NAO index of Jones et al. (1997)) and presents large (AMV) related multi-decadal SST variability. This result suggests that the uptake of CO₂ could be modulated

by NAO with periodicity of nearly 10 years (Nigam et al., 2018), as well as changes in AMV. Fröb et al. (2018) also showed a large increase in DIC (enhanced vertical mixing) during positive NAO conditions (near 60°N, in particular in the Irminger Sea). Along the SURATLANT cruise track, that lies west of the Reykjavik Ridge, the reversal in the SST trend may be slightly delayed (around 2007, Fig. 3a) compared to the basin average. Also the effect of changes in vertical mixing on DIC appears less prominent than further west in Fröb et al. (2018), as it is far from the deep convection areas. However, interannual changes in the party Paykinges Pidge mode waters have been documented (Thierry et al. 2008).

5 deep convection areas. However, interannual changes in the nearby Reykjanes Ridge mode waters have been documented (Thierry et al., 2008) that could influence the change in surface DIC.

Another indirect problem of the increase in anthropogenic emissions to the atmosphere is the decrease in the degree of saturation with respect to calcium carbonate (Ω). Because of changes in the trends of the carbonate system parameters, prediction of the time when surface waters will become undersaturated for aragonite and calcite (Ω <1) is highly uncertain. On one hand, when assuming that the slow decrease in Ω observed over the period 2008–2017 will persist in the future (optimistic scenario), undersaturation of surface waters might not be reached in the next 100 years. On the other hand, when considering the average evolution over the last two decades, undersaturation of surface waters could be reached in about 80 years during winter for both aragonite and calcite (30 and 40 years later during summer for aragonite and calcite, respectively).

- 6As mentioned above, the SURATLANT sampling is not available each year for the reference months of February and July selected for the
 summer and winter trend analysis (Table 1). We first constructed a monthly climatology for each property and each box and used this climatology to complement summer and winter for some years when sampling was missing. The mean seasonal cycles constructed from data collected over the period 1993-2017 (only 2001-2017 for TA) are portrayed in Figure 2. For nutrients (not shown here) the seasonal cycle was described by Reverdin et al. (2018b). The seasonal cycles deduced here from the SURATLANT data represent classical variability observed in the North Atlantic north of 50°N and are coherent with other climatology of the oceanic carbonate system constructed from different data and methods
 (Lee et al., 2006; Takahashi et al., 2009, 2014; Becker et al., 2018). Except for salinity and TA, all properties show a marked seasonality in all
- regions with maxima and minima identified at the same period for boxes B, C, D and E. For the northern box E ($62^{\circ}N-64^{\circ}N$, black lines in Figure 2), we note some short time variability during summer for salinity and TA (minimum in July) that impact the fCO₂, pH and Ω cycles in this region.
- 25 The mean monthly DIC concentration (Fig. 2d) is maximum in winter due to deep vertical mixing, presents a steep decline from April to May when phytoplankton blooms start to occur, and a minimum at the end of summer. The mean DIC concentrations are very similar each month north of 54°N (boxes C, D, E) and significantly lower in the southern region (box B, red line in Figure 2) because salinity is also lower in the south. The seasonal DIC amplitude of around 70-80 μ mol kg⁻¹ in the north is slightly more pronounced in the south of around 90 μ mol kg⁻¹. Given the variability from year to year, the mean seasonal cycles of fCO₂, pH and Ω_{Ar} (Fig. 2e,f,g) show fairly similar variations in all boxes.
- 30 As the alkalinity seasonality is low, the seasonal changes in fCO_2 and pH are anti-correlated and the seasonal variability of Ω is relatively similar to that of pH.

Although the temperature is $+3^{\circ}$ C to $+6^{\circ}$ C warmer in summer compared to winter (Fig. 2a), the seasonal fCO₂ variability is mainly driven by DIC, i.e. the biological production in spring-summer dominates the effect of warming and deep mixing in winter dominates the cooling effect.

35 The seasonal amplitude of fCO_2 that vary between 50 and 70 µatm (Fig. 4e) is much larger than in the atmosphere (around 14 µatm at these latitudes). Consequently, in a climatological view, the NASPG is near equilibrium in winter and a strong CO_2 sink in summer. How and why this CO_2 sink is changing over 1993-2017 will be investigated in the next sections.

3.2 Long-term trend and anthropigenic CO₂

When describing the SURATLANT data-set for 1993-2017, Reverdin et al. (2018b) evaluated the long-term trend of properties over a broad 40 region (50°N-63°N). Using data over 24 years (and all seasons) they estimate an increase in DIC of $+0.77 \mu$ mol kg⁻¹ yr⁻¹, a fCO₂ trend of $+1.9 \mu$ atm yr⁻¹ and a pH decrease of -0.0021 yr^{-1} . Here we re-evaluate these trends in each box (B, CDE merged) and only for summer (July) or winter (February) using observations and reconstructed data as described in section (3.3). The trends for 1993-2017 in each box and season are listed in Table 2 (first lines). The DIC increasing rate ranges between +0.5 to +0.9 μ mol kg⁻¹ yr⁻¹ depending on the season and region. For fCO₂ we evaluate trends ranging between +1.5 and +1.7 μ atm yr⁻¹ and for pH between -0.0016 and -0.0019 yr⁻¹. Not surprisingly, because the same original data are used, the summer and winter trends for each box (B, CDE) are consistent with preliminary results from Reverdin et al. (2018b).

- 5 From 1993 to 2017, we also observed a warming, most pronounced in summer (up to +0.05 °C yr⁻¹, Table 2), but the fCO₂ increase and pH decrease are mainly explained by DIC increase. The long-term fCO₂ and pH changes are thus mainly attributed to anthropogenic CO₂ uptake. This is also supported by a decrease in δ¹³C_{DIC} (Suess effect) along SURATLANT track but for a shorter period, 2005-2017 (Reverdin et al., 2018b), a signal observed at depth in the Irminger Basin between 1981 and 2006 and linked to anthropogenic CO₂ (Racapé et al., 2013).
- 10 To gain insight in the DIC trends and separate natural versus anthropogenic contributions to the fCO₂ and pH trends, we evaluate the anthropogenic DIC (hereafter noted C-ant) in the NASPG region. Here we use the TrOCA method (Tracer combining Oxygen, inorganic Carbon and total Alkalinity, Touratier et al., 2007) applied to data available in the GLODAP-V2 data-base (Key et al., 2015; Olsen et al., 2016). In the NASPG, repeated observations since 1997 were mostly conducted during summer (13 cruises in June-September). Because indirect methods such as TrOCA are not suitable to evaluate C-ant concentrations in surface waters (due to biological activity and gas exchange) we calculate C-
- 15 ant in the layer 150-200m only. For the period 1997-2010, we estimate a C-ant trend of $+0.6 \mu \text{mol } \text{kg}^{-1} \text{ yr}^{-1}$ in the NASPG. The anthropogenic signal would explain 65% of the DIC trend of $+0.9 \mu \text{mol } \text{kg}^{-1} \text{ yr}^{-1}$ observed in GLODAP-V2 subsurface data for the same period. Note that we obtain similar results when selecting different periods (C-ant = $+0.53 \mu \text{mol } \text{kg}^{-1} \text{ yr}^{-1}$ for 1997-2007 whereas it is $+0.58 \mu \text{mol } \text{kg}^{-1} \text{ yr}^{-1}$ when restricted to 2001-2007).
- 20 Recently, a new data-based method, eMLR(C*), developed by Clement and Gruber, (2018) was used to evaluate the accumulation of C-ant from 1994 to 2007 in the global ocean (Gruber et al., 2019a). To compare with our estimates based on TrOCA, we explore the C-ant concentrations from eMLR(C*) in the NASPG (data extracted from Gruber et al., 2019b). Along the SURATLANT line, the accumulated C-ant between 1994 and 2007 is +8.5 (±1.7) µmol kg⁻¹ in the layer 150-200m. This would correspond to a C-ant trend of +0.65 µmol kg⁻¹ yr⁻¹ close to our C-ant estimate based on GLODAP-V2 and TrOCA method in the same layer. This is not surprising as Gruber et al. (2019a,b) used GLODAP-V2 data
- 25 as well. If we assume that the subsurface C-ant trend is also valid for the surface layer, the eMLR(C*) method leads to very homogeneous C-ant accumulation in the layer 0-50m along the SURATLANT line ($55^{\circ}N-64^{\circ}N$), of +10.1 (± 0.8) µmol kg⁻¹ between 1994 and 2007, i.e. about +0.8 µmol kg⁻¹ yr⁻¹. Again, this is in the range of the long-term (1993-2017) DIC surface trends that we report (Table 2) between +0.7 µmol kg⁻¹ yr⁻¹ and +0.9 µmol kg⁻¹ yr⁻¹ in boxes CDE (depending on the season). Interestingly, in the region 55°N-64°N winter DIC from SURATLANT averaged 2134.1 (± 2.8) µmol kg⁻¹ in 1994 and 2145.1 (± 2.1) µmol kg⁻¹ in 2007, i.e. an increase of + 11 µmol kg⁻¹ almost equal to the C-ant
- 30 accumulation deduced from eMLR(C*) over the same period. These independent estimates confirm that in the NASPG the observed long-term DIC trend and derived trends for fCO₂ and pH in surface waters (Table 2, 1993-2017) are mostly linked with anthropogenic CO₂ uptake. The same conclusion was drawn for the subpolar mode waters found in subsurface layers in the NASPG (Vázquez-Rodríguez et al., 2012; García-Ibáñez et al., 2016; Fröb et al., 2018). For example, based on data collected in 1981-2008, Vázquez-Rodríguez et al. (2012) estimated that 75% of the observed pH decrease (-0.0019 yr⁻¹) in the Subarctic intermediate waters (SAIW) in the Irminger Basin is due to anthropogenic DIC.
- 35 García-Ibáñez et al. (2016) incorporating 4 additional cruises (2010-2015) estimated a pH decrease of around -0.0018 yr⁻¹ over 1991-2015 in the subpolar mode waters (SPMW) found around 200-300m in the Irminger basin. They also conclude that in the SPMW the pH decrease is dominated by DIC increase (+0.82 μ mol kg⁻¹ yr⁻¹) though anthropogenic CO₂ (C-ant trend of +0.9 μ mol kg⁻¹ yr⁻¹) but this is modulated by a pH increase over time due to an increase in alkalinity (about +0.11 μ mol kg⁻¹ yr⁻¹). From the SURATLANT time series (1993-2017) we also observe a small increase in TA during winter (+0.1 μ mol kg⁻¹ yr⁻¹, Table 2) coherent with the TA signal observed in the SPMW layer from data collected
- 40 <u>in summer (García-Ibáñez et al., 2016). The TA increase in the SPMW layer in the Irminger basin is directly linked with salinity increase</u> (García-Ibáñez et al., 2016) attributed to advection of higher salinity of subtropical origin and also associated with the contraction of the subpolar

gyre since the mid-90s (Häkkinen and Rhines, 2004). However, we observed much stronger TA increase in surface water during summer, up to $\pm 0.4 \,\mu$ mol kg⁻¹ yr⁻¹ in the northern region (Table 2, box CDE). Such TA increase would lead to a pH change of around ± 0.0009 yr⁻¹, counteracting the impact of DIC increase. In addition, when TA is normalized in salinity, we evaluate summer sTA trends of $\pm 0.2 \,\mu$ mol kg⁻¹ yr⁻¹ in the south (Table 2) suggesting that the TA changes are not solely linked to salinity and advective process.

5

At high latitudes in the open ocean such long-term positive TA trend was only observed (to our knowledge) in the Pacific Western Subarctic Gyre (Wakita et al., 2013, 2017). There, in the winter mixed-layer, Wakita et al. (2017) estimate positive TA and sTA trends of +0.4 and +0.34 µmol kg⁻¹ yr⁻¹ over 1999-2015. This leads to a long-term pH decrease in this region (-0.0008 yr⁻¹) much slower than observed in other open ocean times-series stations (Bates et al., 2014) and in the NASPG for 1993-2017 (Table 2). The TA increase also leads to slow fCO₂ increase

- 10 +0.9 µatm yr⁻¹ (Wakita et al., 2017). Wakita et al. (2017) suggested the TA increase might be due to weakened calcification (but this process was not quantified). Therefore, in addition to advection or convective processes, biological process such as calcification cannot be ruled out to explain TA and sTA long-term positive trends observed during summer in the NASPG (Table 2). At the high latitudes of the North Atlantic blooms of the coccolithophorid (*Emiliania huxleyi*) are well captured from space (Brown and Yoder, 1994) and there is indication that these blooms were more pronounced in the 1990s compared to the last two decades, 2000-2017 (Loveday and Smyth, 2018). Thus, in addition to DIC
- 15 and anthropogenic CO₂, a better knowledge of temporal TA dynamics is relevant for an understanding of fCO₂ and pH changes. It is worth noting that Ocean BioGeochimical Model (OBGM) used to quantify the carbon cycle at large scale are not able to fully capture TA variability when calcifying phytoplankton is not explicitly included (Ullman et al., 2009, who used 1993-2005 SURATLANT data for model comparison). When multiple phytoplankton functional groups including coccolithophores are explicitly parameterized in ecosystem carbon models, the seasonal cycle of both DIC and TA are better represented in the NASPG (Signorini et al., 2012). The same is likely true to interpret inter-annual to decadal TA variability and explain the drivers of observed fCO₂ and pH trends along SURATLANT line.

Because the variability in summer is much more pronounced at high latitudes due to low stratification and primary production often encountered at meso-scale, most studies focused on winter to analyze and interpret the decadal trends of the carbonate system in surface waters (Olafsson et al., 2009; Metzl et al., 2010; Fröb et al., 2019; Omar et al., 2019). Only few observational studies conducted at high latitudes showed that the

- 25 trends of DIC, fCO₂ and pH are seasonally different and thus driven by different processes not yet fully explained. In a global context, taking into account a seasonal view for the trend analysis is also relevant to better understand the strengthening of fCO₂ seasonality observed over the last 3 decades (Landschützer et al., 2018) and how this would change the degree of acidification in the future (Kwiatkowski and Orr, 2018). Note that the observed trend of fCO₂ seasonality (winter minus summer) in the North Atlantic appears less pronounced than in other regions with significant sub-decadal variability (see Fig. 1b and Fig. 4a in Landschützer et al., 2018). In this context we now investigate the observed
- 30 trends for winter and summer in more detail and over specific periods to quantify the effect of temperature, salinity, DIC, TA that drive the fCO₂ and pH variations in the NASPG.

The periods 1993-1997, 2001-2007 and 2008-2017 are selected for several reasons. First, as the trends and quantification of drivers are sensitive to the data selection we only select periods when time series for carbonates data were conducted (e.g. no DIC and TA data available in 1998-2000, see Table 1). This is in contrast with previous work where trends based on SURATLANT data were evaluated over 1993-2003 (Corbière et al., 2007; Metzl et al., 2010). Second, we use a new binned products based on more regular SST and SSS observations (Reverdin et al., 2018a) to separate periods that present significant inter-annual variability and different trends in temperature and salinity (Fig. 3a,b). Finally, in the NASPG it is well recognized that decadal and multidecadal variability in temperature, salinity, winter convection and large scale gyre circulation are associated with the phase of NAO or AMO (Fig. 3c).

40

During the first observational period 1993-1997 (rather short), NAO shifted from a positive to negative phase while AMO was in a transitional stage and regularly increased during the nineties (Fig. 3c). During the positive NAO in the early 90s, the NASPG experienced deep convection

regime in the western subpolar gyre (Pickart et al., 2003). During the second period 2001-2007, NAO was negative or neutral and AMO reached a high index. The convection in the western NASPG was relatively shallow during this period and the ocean surface warmed (Fig. 3a). In the last decade, 2008-2017, NAO was highly variable compared to previous periods, with lowest phase in 2010 and highest phase in 2015 (Fig. 3c). On the opposite, AMO strongly decreases since the late-2000s. During this period, both SST and SSS anomalies present clear negative trends:

5 the NASPG becomes colder and fresher (Fig. 3a,b) during this period also associated with several deep convection events occurring in the western subpolar gyre during the winters 2008, 2012 and 2015 (Våge et al., 2008; de Jong and de Steur, 2016; Fröb et al., 2016; Piron et al., 2017).

3.3 Winter trends at different periods

The trends and drivers in winter are identified in blue symbols in Figures 4 and 5. During the first period, 1993-1997 the results are contrasted between the southern and northern regions. The strongest change occurs in the south (box B), where we observe a rapid cooling over 4 years (- $0.19 \,^{\circ}$ C yr⁻¹), an increase in salinity (+0.045 yr⁻¹) and an increase of TA (+2 µmol kg⁻¹ yr⁻¹) that is directly linked to salinity (recall that for 1993-1997 TA was not measured and the TA values are based on Salinity, Eq. 1). Over this short period, this leads to a strong decrease of fCO₂ (-7 µatm yr⁻¹) and an increase in pH both attributed to the cooling and TA changes (Fig. 5a,d), the effect of DIC being minor. In the north (boxes CDE), we do not observe any significant trend of winter properties in 1993-1997 for SST, sTA, sDIC, pH and fCO₂. As a result, in the NASPG

15 (all region), the oceanic fCO_2 trend does not follow the atmospheric CO_2 increase and the air-sea disequilibrium increases, i.e. the region was a CO_2 source in winter 1994 and reached near-equilibrium afterwards (Fig. 4h).

As opposed to the nineties, data collected in winter during the second period (2002-2007) show a gradual DIC increase in the two regions (+1.7 and +2.1 μ mol kg⁻¹ yr⁻¹, Table 2) higher than expected from anthropogenic CO₂ increase. A decrease in TA is also observed in the northern

- 20 region but not directly related to salinity. This leads to significant pH decrease (-0.006 to -0.008 yr⁻¹) and fast fCO₂ increase (+6 to +7 μ atm yr⁻¹). For this period, the DIC increase explains the temporal changes of pH and fCO₂ in box B, whereas both DIC and TA drive these changes in box CDE (Fig. 5b,e). In contrast to 1993-1997, the winter oceanic CO₂ source increases during 2002-2007. It is near equilibrium in 2002 and a source in 2004-2007 (Fig. 4h) a result previously confirmed with independent sea surface fCO₂ observations (Metzl et al., 2010). At the end of this period, in winter 2007, oceanic fCO₂ was higher than 400 μ atm and pH was low, near 8.04.
- 25

The last period, 2008-2015, was not investigated in previous studies (Corbière et al., 2007; Metzl et al., 2010). During 2008-2015, the DIC concentrations in winter continue to rise (+1.0 to +1.3 μ mol kg⁻¹ yr⁻¹, Table 2) but at a slower pace compared to previous years and still higher that the anthropogenic DIC trend. As opposed to 2001-2007 we do not observe large changes in TA. In the northern region (box CDE) the sea surface cools (-0.05 °C yr⁻¹), which is not found in the southern region, inducing different fCO₂ and pH trends in the southern and northern

- 30 sectors. In the north, the low fCO_2 and pH trends are due to DIC increase compensated by cooling and a small TA increase, whereas in the south the fCO_2 trend (+2.5 µatm yr⁻¹) and pH trend (-0.0024 yr⁻¹) are mainly driven by DIC increase (Fig. 5c,f). These trends deviate from the ones in 2001-2007 with different processes possibly related to NAO presenting much more variability during the last period (Fig. 3c). At the end of our time-series and in both regions fCO_2 in winter 2015 reaches the highest value (410 µatm) recorded since 1993, pH the lowest values (8.03) and the same for Ω_{Ar} (1.7). This is mainly explained by DIC concentrations approaching 2160 µmol kg⁻¹ in February 2015 (Fig. 4e). These high DIC
- 35 concentrations observed in winter 2015 correspond to a high positive NAO phase (Fig. 3c) and correspond to negative SST anomalies (Fig. 3a). It was also associated with strengthening of fresh water coming from of the western NASPG (Holliday et al., 2019), and likely resulted in increased vertical mixing over the Reykjanes Ridge (De Boisséson et al., 2012). The high DIC and sDIC concentrations observed in winter 2015 are not unique to the Irminger Sea. Recently, based on sea surface fCO₂ measurements conducted in winter 2004-2017 and DIC calculated from fCO₂ data and reconstructed TA (using adapted TA/SSS relation), Fröb et al. (2019) report average winter sDIC concentrations of around 2160
- 40 μmol kg⁻¹ in 2012 and 2014. These authors also observed high sDIC concentrations in winter 2017, above 2165 μmol kg⁻¹. Unfortunately, we cannot compare these values as we have no winter data after 2015 along the SURATLANT line (Table 1). Although the periods are not exactly

the same and methods to evaluate trends are different, the sDIC trends reported by Fröb et al. (2019) are in the same range as here: between +1.3to $+1.75 \mu$ mol kg⁻¹ yr⁻¹ for the period 2004-2017, when our results in the north (i.e. boxes CDE including the Irminger Sea) lead to a sDIC trend of $+1.8 \mu$ mol kg⁻¹ yr⁻¹ for 2001-2007 and $+1.3 \mu$ mol kg⁻¹ yr⁻¹ for 2008-2015 (Table 2). Both results show a clear increase of sDIC in the NASPG or Irminger Sea since 2001 (or 2004), and the differences in trends might be also modulated by inter-annual variability.

5

During 2008-2015 we also observe significant inter-annual variability in winter, with marked DIC minima in 2010 and 2013 also seen in sDIC concentrations as well as in TA and sTA (Fig. 4c,d,e,f). Interestingly, Fröb et al. (2019) also report lower sDIC concentrations in 2010 and 2013 in the Irminger Sea. In 2010, NAO shifted to a negative phase (Fig. 3c) supporting relatively shallow convection in the NASPG and inducing positive SST anomalies (Fig. 3a); the absence of deep mixed layers during these years would explain the relatively low DIC and TA

- 10 concentrations observed in winter (i.e. less input of high DIC and TA from subsurface layers). In 2013, although the NAO was neutral we also observed lower DIC and TA in winter. It is suggested that mixing was relatively shallow in the Irminger Sea and near the Reykjanes Ridge in 2013, which could drive less renewal of the surface layers by the enriched sDIC deeper waters, and thus negative winter DIC and TA anomalies for this particular year. However, as both DIC and TA decrease, fCO₂ and pH are not strongly changing for these particular years (2010 and 2013) and associated air-sea CO₂ disequilibrium remains stable (Fig. 4h). The strong negative DIC anomalies observed in 2010 and 2013
- 15 nonetheless influence the DIC trend for the period 2008-2015: not including those two years increases the trend in boxes CDE from $\pm 1.0 \,\mu$ mol kg⁻¹ yr⁻¹. However, this is still lower compared to 2002-2007 ($\pm 1.7 \,\mu$ mol kg⁻¹ yr⁻¹) and thus much slower trend for fCO₂ and pH are estimated in recent years. As a result, in 2008-2015 we interpret the fCO₂ and pH winter changes equally due to the contribution of anthropogenic CO₂ (C-ant) and the natural component (DIC-nat), whereas in 2001-2007 the natural component dominates attributed to the dynamics in the NASPG (Fig. 6c,d).

20 <u>3.4 Summer trends at different periods</u>

We examine the trends and drivers in summer over the same periods selected for winter (except for the last decade, 2001-2017 in summer and 2002-2015 for winter). Results for summer are identified by red symbols in Figures 4 and 5. As mentioned above, trend analysis in summer was not performed in previous work based on SURATLANT data (Metzl et al., 2010). Here we attempt for the first time to detect trends and processes occurring during this season and how they impact fCO₂, air-sea CO₂ equilibrium and pH changes. Not surprisingly, the temporal variability of

- 25 the carbonate properties is much more pronounced during summer when biological processes generally starting in spring imprint large DIC variations at seasonal scale (Fig. 2). The biological bloom and its timing may also lead to significant inter-annual variability but as we use July as a reference for summer, we expect to record each year the low DIC concentrations due to accumulated carbon uptake though production occurring in spring-summer.
- 30 During the first period, 1993-1996, the most remarkable feature is a very rapid increase of DIC in the northern and southern sectors (+4 and + 9 μ mol kg⁻¹ yr⁻¹). This contrasts with the DIC trends in winter over 1994-1997 (Table 2). Because the northern box (CDE) also experienced a sharp warming of +0.6 °C yr⁻¹, there the fCO₂ increase (+12 to +14 μ atm yr⁻¹) and pH decrease (-0.015 to -0.017 yr⁻¹) are particularly fast but we admit the period is too short to clearly interpret which are the main processes at play and derive any conclusion on the trends. We notice that the NAO changed from a positive to negative phase in 1993-1996 and AMO progressively increased in the nineties (Fig. 3c) but no particular
- 35 anomalies were revealed in the winter observations. Thus we have no straight explanation for the fast DIC, fCO_2 and pH changes observed during the summers 1993-1996, except that relatively higher DIC in 1996 might have resulted from a decrease in primary production compared to previous years. This is rather speculative as we have no other information on biological component (e.g. from remote sensing at the beginning of the nineties). The fCO_2 data show that the region was a large CO_2 sink in summer 1993-1995 but abruptly raised to near-equilibrium values in 1996 (Fig. 4h). In the northern region (box CDE), the mean delta- fCO_2 value in summer 1996 was close to 0 µatm, i.e. about the same as
- 40 observed during the winter 1996-1997.

The SURATANT regular sampling for DIC, TA and nutrients was restarted in June 2001 (Table 1). During 2001-2007, and as in summer 1993-1996, we observe a rapid increase of fCO_2 (+8 to +12 µatm yr⁻¹) and pH decrease (-0.010 to -0.013 yr⁻¹). The summer DIC and TA trends in the northern and southern areas have the same sign (similar as during winter), positive for DIC and negative for TA but not directly related to salinity (Table 2). However, the DIC increasing and TA decreasing rates are regionally significantly different. The DIC increase is most pronounced in

5 the north (+5 μ mol kg⁻¹ yr⁻¹) and the TA decrease more pronounced in the south (-3.9 μ mol kg⁻¹ yr⁻¹). Although the fCO₂ and pH trends are similar in the two areas, this suggests different drivers for boxes B and CDE (Fig. 5b,e). In the north, DIC explains most of the fCO₂ and pH change, whereas in the south it is TA contribution that dominates. In both regions, as in winter, temperature and salinity changes have a small effect for this period (Fig. 5b,e). The rapid oceanic fCO₂ increase strongly impacts the variations of air-sea CO₂ disequilibrium (Fig. 4h). In the north, the region was a sink in 2001-2004 but reaches equilibrium in 2005 and 2007 (no data in July 2006 in the north). In July 2007, temperature

10 was relatively low (around 10°C) and the high fCO₂ at that period was mainly due to high DIC concentrations either linked to low productivity that year or linked to deeper mixing that occurred that year when NAO moved to a positive phase (Fig. 3c).

For the last period, 2008-2017, results in summer are very different compared with previous decades as we now observe a decrease of fCO_2 and an increase of pH in both regions (Fig. 4g,i; Table 2). This also contrasts with the winter trends in 2008-2015. The variation of fCO_2 leads to a

15 strong ocean CO₂ sink with low delta-fCO₂ in 2010-2017 (-40 to -80 µatm, Fig. 4h). During the summers 2008-2017 sea surface properties are very variable that might be related to the NAO variability in this period (Fig. 3c), but also to changes in the ship's route in some years or to productivity occurring at meso-scale. This was the case in July 2013 where the sampling took place further north-west (Fig. 1), impacting SST (colder, Fig. 4a) and DIC (stronger, Fig. 4 e,f). However these anomalies are less noticable on fCO₂ and pH (Fig. 4g, i) because the effects of SST and DIC partially compensate. Thus, we chose to not consider July 2013 for calculating trends and drivers.

20

Although the inter-annual variability is large in summer, the trends are evaluated over the period 2008-2017 using all available data (except July 2013). For this period all terms (SST, DIC and TA) contribute to the fCO₂ and pH changes (Fig. 5c,f). The DIC increase is only revealed in the north (box CDE, +1.2 μ mol kg⁻¹ yr⁻¹); this is slightly higher than in winter (+1.0 μ mol kg⁻¹ yr⁻¹) and thus higher than anthropogenic signal (around +0.6 μ mol kg⁻¹ yr⁻¹). However, as the surface ocean cools (-0.11 °C yr⁻¹) and TA increase (+1.7 μ mol kg⁻¹ yr⁻¹), the net effect is a

25 decrease of fCO₂ (-2.3 µatm yr⁻¹) and pH increase (+0.0026 yr⁻¹). During 2008-2017, the progressive cooling in the NASPG, reflected here in both winter and summer data (Fig. 4a) is a large-scale signal (Fig. 3a, Robson et al., 2016; Reverdin et al., 2018a), suggesting that our discrete sampling for DIC and TA records relevant changes of biogeochemical properties in this region. An intriguing signal in 2008-2017 is the increase of TA (Fig. 4c) opposed to the decease of salinity (Fig. 3e, Fig. 4b); this leads to positive sTA trend opposite to summer 2001-2007. Therefore we cannot interpret the observed TA increase directly linked to salinity. The shift of the sTA trend, negative in 2001-2007 and positive in 2008-2017.
2017. Increase directly linked to salinity. The shift of the sTA trend, negative in 2001-2007 and positive in 2008-2017.

30 <u>2017</u>, is an important signal that drives opposite trends for fCO_2 and pH between the two periods (Fig. 5b,c,e,f).

This contrasting TA signal in summer cannot be attributed to error or drift in laboratory analyses as the measurements were performed using the same technics over years (Reverdin et al., 2018b) and no such signal is identified for winter cruises in 2008-2015. In addition, during OVIDE cruises conducted in summer 2006-2014 in the North Atlantic (e.g. García-Ibáñez et al., 2016), we performed regular TA and DIC inter-

35 comparisons with the ICM/CSIC group in Vigo (F. Pérez) and certified our results to within around $\pm 4 \mu$ mol kg⁻¹ both for TA and DIC. Results based on the surface TA samples measured at LOCEAN for the OVIDE cruises in summer 2006-2018 (data in Metzl et al., 2018) also suggest that sTA increases in the NASPG at a rate of around +1.5 µmol kg⁻¹ yr⁻¹.

To support these results, we have evaluated sTA trends in the NASPG from independent data available in the most recent GLODAP-v2019 40 version (Olsen et al., 2019). For this we selected the data in the layer 0-20m for all cruises conducted in June-August in 1997-2014. We found a significant difference of sTA trends during this period: -0.52μ mol kg⁻¹ yr⁻¹ in 1997-2006 against +0.54 µmol kg⁻¹ yr⁻¹ in 2006-2014. Although the periods are not exactly the same and sTA trends from GLODAP-v2019 are smaller than those deduced from the SURATLANT time-series, the changing sTA trends from negative to positive in recent years also features in that dataset. We are thus confident with TA data over time and need to find a process that explains why the sTA trend was negative in summer 2001-2007 (-1.9 μ mol kg⁻¹ yr⁻¹) and positive in summer 2008-2017 (+2.3 μ mol kg⁻¹ yr⁻¹).

- 5 The variability of calcification through the production of calcifying species (e.g. coccolithophores, foraminifera) is a possible mechanism that would impact on TA trends as suggested by Wakita et al. (2017) in the Pacific Western Subarctic Gyre. In the North-East Atlantic, long-term in-situ CPR observations (Continuous Plankton Recorder) showed a significant increase of the calcifying species starting in the mid-90s (Beaugrand et al., 2013). These authors suggest that the temperature (a warming) was the main driver of the positive trend of calcifying plankton. In addition they show that no correlation was identified between the NAO and species variability but that positive trend of the calcifying species
- 10 were correlated with AMO, a result also confirmed by Rivero-Calle et al. (2015). The TA decrease in summer we observe during the period 2001-2007 after the AMO moved to its positive state (Fig. 3c), might be explained by the increase of calcifying species as identified from insitu CPR observations in the North Atlantic (Beaugrand et al., 2013; Rivero-Calle et al., 2015). Unfortunately, we don't have yet direct in-situ observational evidence of a reduced calcifying species after 2010. However if one follows the proposed scenario for 2001-2017, the TA increase in summer 2008-2017 during the cooling phase in the NASPG could be linked to a weakening of calcification. In this region, this seems supported
- 15 by the absence of coccolithophores blooms in recent years (2010-2017) as identified from remote-sensing reflectance records (Loveday and Smyth, 2018).

4 Discussion

Our observations collected over the last three decades show an abrupt change in the evolution of hydrological and biogeochemical properties in the NASPG around the year 2007 (Fig. 4) when AMO reached a maximum and NAO was around neutral (Fig. 3c). Following a warming since

- 20 the mid-90s, the region experienced a large cooling and freshening after 2005 (Fig 3a,b; Robson et al., 2016; Holliday et al., 2019). This change is associated with an increase in the size of the gyre and increased currents along the gyre southern rim (Chafik et al., 2014, 2019; Desbruyères et al., 2015), as well as by a very large heat loss during positive NAO years particularly in 2015 (Fig 3c, Josey et al., 2018). Indeed, NAO was previously recognized as a possible cause of the rapid fCO₂ increase when NAO shifted from positive to negative phase in 1995-1996 (Fig. 3c; Corbière et al., 2007). However, this was not confirmed for the period 2001-2007 when NAO did not vary so much around a neutral value (Fig.
- 25 <u>3c</u>; Metzl et al., 2010). For the whole NA, Schuster et al. (2009) synthetized fCO₂ observations over 1990-2006, i.e. before 2007 when we observe abrupt changes in property trends. North of 45°N, Schuster et al. (2009) evaluate a trend of fCO₂ exceeding $+3 \mu$ atm yr⁻¹ and a significant decrease of the CO₂ sink in the NA by over 50% between 1990 and 2006. They also predict an increasing sink in the subpolar regions following the increasing NAO index in 2007. Although the impact of the climatic modes (NAO and/or AMO) on the oceanic physical properties and circulation has been well established, their effects, if any on the fCO₂ and pH trends need to be clarified.
- 30

Whatever the NAO variability, the long term fCO_2 and pH trends we evaluate over 1993-2017 in the NASPG for summer or winter are mainly explained by the increase in DIC associated with the uptake of anthropogenic CO_2 (Fig. 6), that is the DIC or sDIC trends (Table 2) are not significantly different from the anthropogenic DIC trend estimated between 1994 and 2007 in this region (Gruber et al., 2019a). For fCO_2 , here calculated from DIC/TA pairs, the long-term trends between +1.5 to +1.7 µatm yr⁻¹ in the NASPG (Table 2) are slightly higher than the mean

- 35 trend of +1.47 (± 0.06) µatm yr⁻¹ evaluated for 1992-2014 in the whole NA (Lebehot et al., 2019) based on monthly reconstructed fCO₂ using a Multiple Linear Regression (MLR) approach and SOCAT-v4 fCO₂ data (Bakker et al., 2016). Lebehot et al. (2019) show that the fCO₂ trends based on observations are much lower than those derived from 19 ESM CMIP5 models, +1.90 (± 0.09) µatm yr⁻¹. By performing several sensitivity test analyses on the ocean ESM models, Lebehot et al. (2019) conclude that the discrepancy between observed and simulated fCO₂ trends originates mainly in model's biogeochemistry, e.g. biases in simulated TA. This might be especially relevant for the NA subpolar region
- 40 where some ESM models project faster change of ocean fCO₂ in the future (2061-2100) with 60% due to the DIC increase and up to 29% due

to the TA changes (Tjiputra et al., 2014). We also suspect that ESM models used to predict future change of the oceanic CO_2 sink and ocean acidification would produce faster pH trends than what we observed.

If the long-term fCO₂ and pH trends could be mainly explained by anthropogenic CO₂ uptake in the NASPG, at shorter time scales (4-10 years)

- 5 the trends are very different (Table 2). Indeed, the gradual changes of fCO₂ and pH caused each year by the uptake of anthropogenic CO₂ can be significantly masked by the natural variability of DIC (DIC-nat), temperature and/or TA. To better identify when and why the DIC-nat dominates we separately compute the impact of anthropogenic CO₂ (C-ant) and DIC-nat on pH and fCO₂ trends for each season and periods. The results for pH are synthetized in Figure 6. The same results are obtained for fCO₂ (not shown), with an opposite sign for each bar plotted on Figure 6. For C-ant we adopt a value of +0.6 µmol kg⁻¹ yr⁻¹ as described in section 3.2.
- 10

For all sub-periods and both seasons, the effect of DIC-nat on pH trend is significant and with similar or higher magnitude than the effect of Cant (Fig. 6). Occasionally it opposes C-ant, i.e. DIC-nat decreases with a positive effect on pH trend (Box B, 2008-2017 in summer, Fig. 6a and Box CDE, 1994-1997 in winter, Fig. 6d). Over 1993-1997 the DIC-nat effect on pH trends for this short period is opposed in summer and winter, suggesting that this is not linked to changes in regional circulation, e.g. less or more input of DIC from different water masses. For 1993-1997 the largest DIC nat effect being observed in summer (in the perthern and southern boxes) one might suggest that it is linked to primery

15 the largest DIC-nat effect being observed in summer (in the northern and southern boxes), one might suggest that it is linked to primary productivity; unfortunately, prior to SeaWIFS in 1998, we have no direct or indirect information on biological changes to explain why DIC-nat increased in summer 1993-1997. However, the length of this period is short to interpret trends highly sensitive to the starting and ending years.

- Apart for the first short period (1993-1997) the largest effect of DIC-nat is observed in summer 2001-2007 in the northern region (Fig 6b). This
 period includes a decade (1995-2005) where the strength of the subpolar gyre circulation decreased (Häkkinen and Rhines, 2004, 2009; Häkkinen et al., 2011, 2013) suggesting that more water of subtropical origin penetrates in the NASPG. This would have decreased the DIC surface concentrations (and increase TA as well), but for 2001-2007 we observed the opposite, including in winter (Table 2). We thus eliminate the effect of advection to interpret the DIC-nat increase in the NASPG that impacts significantly on pH trend. As mixed-layer depths are not deeper than 30-40m in summer and present no significant inter-annual changes (analyses done using the dataset Armor which presents the same
- 25 variations as the data of product Global Reanalysis PHY 001 030 present on http://marine.copernicus.eu/), the variation of the vertical mixing during this season is not a likely candidate to explain the changes of DIC-nat. A possible explanation for the large contribution DIC-nat on pH (and fCO₂) trend in 2001-2007 could be a decline in biomass as identified in SeaWIFS data in the eastern subpolar region for years 1998-2007 although the trends for net primary productivity (NPP) appears not statistically significant over 10 years (McKinley et al., 2018). For the NPP subject to high frequency variability the evaluation of trends over nearly 10 years is challenging. Annual biomass anomalies (based on SeaWIFS)
- 30 and MODIS sensors) moved from positive values in 1998-2004 to negative in 2005-2009 (McKinley et al., 2018). To explain the biomass decline McKinley et al. (2018) used a coupled physical biogeochemical ocean model (OBGM) to reproduce these changes and found that nutrient concentrations decline significantly in the region north of 50°N due to reduced physical supply through horizontal and vertical fluxes; their model suggests that enhanced phosphate and silicate limitation over time dominates the light limitation in this region.
- 35 Due to limited sampling months and the high variability of nutrients in spring-summer we have not been able to detect such mechanism from the SURATLANT nutrient data. However, the reduced productivity due to nutrient limitations (McKinley et al., 2018) is supported by independent observations of silicate concentrations synthetized in the subpolar NA over 25 years. Hátún et al. (2017) showed a decline in prebloom silicate concentrations in the winter mixed layer since the 1990s until 2010 and attributed the remarkable silicates changes to the decrease in winter convection depth and the weakening of the NASPG. This decline of silicates observed over 25 years would negatively impact diatom
- 40 blooms in spring and favor coccolithophore blooms occurring in summer. Such scenario is coherent with the increase in calcifying species since the mid-90s as observed from the CPR data in the NA during a warm period associated to the AMO (Beaugrand et al., 2013; Rivero-Calle et al., 2015). The shift of phytoplankton species and local or regional intensified calcification might also explain the low sTA concentrations

occasionally observed in 2003 and 2005, i.e. lower than for summer 2001 and also for winter (Fig. 4d). The inter-annual variability of TA of around $\pm 8 \mu$ mol kg⁻¹ in 2001-2007 is twice the TA change of $\pm 4 \mu$ mol kg⁻¹ due to coccolithophores in a biological model applied at 60°N-30°W (Signorini et al., 2012). The TA and sTA negative trends observed in 2001-2007 (Table 2) contribute less to pH and fCO₂ trends than with DIC (Fig. 5b,e), but nearly the same magnitude compared to the contribution of C-ant. This is not the case after 2007.

5

During the last decade, 2008-2017, observations were obtained during a strong negative NAO in 2010 and a positive NAO phase in 2015 (Fig. 3c). NAO presents large inter-annual variation compared to 1995-2007 (Fig. 3c) and a decline in AMO index after 2010 (Fig. 3c). The 2010 event was associated with a warming and freshening (Fig. 4a,b) found in both SURATLANT discrete sampling (in August 2010) and monthly reconstructed Binned products (Reverdin et al., 2018a). In August 2010 the DIC concentrations were very low in the north (< 2070 µmol kg⁻¹)

- 10 compared to all years since 1993 (Fig. 4e). This was not associated with particular signals in TA but to high $\delta^{13}C_{DIC}$ as reported in Racapé et al. (2014) and also to higher Chl-a concentration identified from MODIS data (McKinley et al., 2018). The effect of the higher productivity in summer 2010 is to lower fCO₂ and increase pH compared to previous summers. Consequently, there is a rapid drop in delta-fCO₂ in 2009-2010: summer 2010 was a strong CO₂ sink. In 2015, when NAO was in a positive phase, the SST anomaly was around -1°C (Fig. 3a): for that year, DIC was high in winter, close to the maximum observed in winter in our time series (Fig 4 e, f). As the temperature also lowers fCO₂, the fCO₂
- values (and pH) were not so different from other winters, illustrating the competing effects of cooling and deeper vertical mixing on fCO₂. Although significant changes are observed on DIC variability during NAO events in 2010 and 2015, this seems to have a small impact on the trends. After 2007 the positive DIC trends are less important than in 2001-2007 (Table 2) and the contributions of the natural and anthropogenic parts of DIC have a similar magnitude in summer and winter (Fig. 6). This result alone does not explain the decrease of fCO₂ and the increase of pH observed during the last period in summer. Indeed, there is also a significant impact of cooling and as opposed to 2001-2007, an intriguing increase in TA, both leading to decreasing fCO₂ and increasing pH trends (Fig. 4; Fig. 5).

<u>5</u> Conclusion and perspectives

The aim of this study was to pursue the study by Metzl et al. (2010) and Reverdin et al. (2018) by evaluating the evolution of the parameters of the carbonate system in surface waters of the NASPG (known as one of the main sinks for anthropogenic CO₂) using data collected over the last three decades, and to better understand the mechanisms responsible for these evolutions. Our study shows a change in the trends around 2007
during both summer and winter for pH and fCO₂, which led to an increase in the ocean capacity to absorb atmospheric CO₂ in the last decade, a near stagnation of pH and the slowdown of the decline in Ω (carbonate ion concentration) in surface waters. This abrupt change in the evolution of the parameters of the carbonate system, which could be due to a change in the gyre circulation (inducing changes in the evolution of DIC, SST and TA), followed a period with a rapid increase in fCO₂ and decrease in pH during both summer and winter starting around the year 2001 (this study, Metzl et al., 2010), following a period with a rapid increase in fCO₂ and decrease in pH during both summer in the 1990s (this study).
Such a multi decadal variability in hydrological and biogeochemical properties of the NASPG makes it difficult to predict the future evolution of CO₂ uptake and ocean acidification, which advocates for the continuation of long term monitoring programs in this region. More regional studies are also needed in order to understand the evolution of the parameters of the carbonate system in different areas of the North Atlantic Ocean, where contrasted changes may occur. In addition to ship based observations, the analysis of data from BGC Argo floats equipped with pH sensors (together with temperature and salinity sensors, from which TA, DIC and fCO₂ can be estimated) will help to better constrain spatial,

35 seasonal and interannual variability.

Based on sea surface observations of DIC and TA collected in the NASPG over 1993-2017 we have analyzed the variability and trends of the 40 carbonate system properties including fCO₂, pH, Ω_{Ar} and Ω_{Ca} calculated from the DIC/TA pairs. This study extends to summer and for pH and

Data availability. The data set is freely available and is accessible at http://www.seanoe.org/data/00434/54517/ (http://doi.org/10.17882/54517, Reverdin et al., 2018b).

 Ω_{Ar} previous work based on winter data (Corbière et al., 2007; Metzl et al., 2010). It also extends the analysis for the last decade, 2008-2017, after the AMO reached a maximum and then decline and when the NAO was highly variable.

In the last decade we observed a continuous surface DIC increase in winter in the northern and southern NASPG. In February 2015 when the NAO was in a positive state, DIC reaches a maximum concentration (DIC > 2150 μmol kg⁻¹, i.e. more than +20 μmol kg⁻¹ higher than in the 90s). In 2015 pH was at minimum (8.03) and fCO₂ was at maximum above 400 μatm and close to the atmospheric fCO₂. Such high fCO₂ was also observed in the NASPG in Jan-Feb 2015 from direct underway measurements (range 405-415 μatm for cruises AGFO20150115 and AGFO20150212 in SOCAT-V5, Bakker et al., 2016). As opposed to the wintertime DIC continuous increase observed since the 90s, the TA decadal variability is not uniform. In 2001-2007 the decreasing of TA, added to the DIC changes, reinforced a rapid fCO₂ increase in up to +7
μatm yr⁻¹ and a strong pH decline of around -0.007 yr⁻¹ confirming previous studies (Metzl et al., 2010). On the opposite, in 2008-2015 the

increasing TA and the cooling in the northern NASPG compensated the effect of DIC increase, leading to much smaller winter trends for fCO_2 and pH, on the order of +1 µatm yr⁻¹ and -0.001 yr⁻¹ respectively.

In summer, the inter-annual variability of all properties is much more pronounced due to active primary productivity in the NASPG in springsummer and shallow mixed-layers. Consequently, the decadal trends of the carbonate system properties in summer are more difficult to detect compared with winter or other oceanic regions such as the subtropics (Bates et al., 2014; Ono et al., 2019). In addition, primary production often occurs at small spatio/temporal scales and the DIC/TA heterogeneous sampling may have occasionally missed planktonic blooms. In 2001-2007 the summer trends of SST, DIC and TA has the same sign as in winter. This confirms the fast increase of fCO₂ and the strong decline of pH observed during this period. The natural variability of DIC dominates the effect of the anthropogenic uptake on fCO₂ and pH trends, especially in the northern region (Fig. 6). The DIC increase in summer is likely due to a reduced productivity during this period (Tilstone et al., 2014; McKinley et al., 2018). After 2007, the fCO₂ and pH trends for summer are drastically different from the previous decade. In both southern and northern parts of the transect, the fCO₂ trend becomes negative while the pH trend is positive (up to +0.016 yr⁻¹ in the south). This is driven by a complex interplay of cooling (-0.1 °C yr⁻¹), DIC increase and significant increase of TA more pronounced in summer than in winter. Such

large changes in pH trends from one decade to another would not have been resolved when using fCO₂ data and TA/S relation instead of TA
 measurements, and support the need to couple DIC and TA measurements in time-series.

Before 2007, we evaluate a rapid fCO_2 increase faster than in the atmosphere. Consequently, the ocean CO_2 uptake decreased in the NASPG from 1993 to 2007 coherent with other studies (Schuster et al., 2009; Landschützer et al., 2013). However, at larger scale, here for the NA-SPSS regional biome (Fay and McKinley, 2014), the decreasing CO_2 sink in the NASPG for this period is not always resolved from fCO_2 data-based

- 30 methods that evaluate an increasing CO_2 sink in the North Atlantic Subpolar region (Rödenbeck et al., 2015; Denvil-Sommer et al., 2019). This disagreement might be in part due to missing fCO₂ data for the period 1994-2003 in the NASPG (Bakker et al., 2016) and need to be investigated in further studies. After 2007, our results show that winter fCO₂ increases at a lower rate than in the atmosphere whereas in summer we observe a decrease of fCO₂. Thus, the ocean CO₂ sink increases over 2008-2017 (Fig. 4h). For this period this is coherent with the results derived from data-based methods in the NA-SPSS biome but only for 2007-2013. Indeed after 2013 the indirect methods produce either an increasing CO_2
- 35 sink or a decreasing CO_2 sink and with a very high variability noticeable in 2015 when the NAO was positive (Fig. S5h in Denvil-Sommer et al., 2019).

The observed change of all sea surface properties around year 2007 in the NASPG, as well as a decreasing CO_2 sink before 2007 and an increasing CO_2 sink after 2008 (Fig. 4h) seems rather linked to the AMO than directly to NAO (Fig. 3c) as also suggested from data-based

40 reconstructed fCO₂ fields in the North Atlantic (Landschützer et al., 2019).

The temporal change of fCO_2 and CO_2 uptake around 2007 that we deduce from SST, DIC and TA, is also clearly observed in pH variability. In summer, the rapid pH decline in 2001-2007 is followed by a significant pH increase in 2008-2017. This is due to a changing trend in TA that was negative before 2007 and positive after 2008, a signal observed in both seasons. This unexpected decadal change in TA, also observed in the North-Western Subpolar Pacific might be linked to changes in calcification processes (Wakita et al., 2017). Indeed, it has been recognized

- 5 that calcifying species in the North Atlantic present significant variations since the mid-90s (Beaugrand et al., 2013). To quantify how this process impacts fCO₂ and pH variability deserves further studies to investigate the coupling of chemical measurements with species observations such as obtained from CPR in the NASPG.
- Although we identified significant inter-annual to decadal variability in surface carbonate system properties over the full time-series (1993-2017) the long-term trends of fCO₂ and pH in winter and summer are almost entirely explained by the DIC increase and anthropogenic CO₂ uptake (Fig. 6). The long-term trend of fCO₂ in the NASPG (between +1.5 and +1.7 μ atm yr⁻¹) is slightly higher than the mean value (+1.47 μ atm yr⁻¹) evaluated for 1992-2014 at large scale in the NA (Lebehot et al., 2019). Our results now extended to 2017 confirm the fCO₂ trends evaluated by McKinley et al. (2011) for the period 1981-2009, and our new estimate for 1993-2017 in summer (+1.7 μ atm yr⁻¹) is not significantly different from the trend of +1.8 μ atm yr⁻¹ estimated for 1981-2002 based on a few observations in August (Corbière et al., 2007). However, it is
- 15 worth noting that in other NA sectors and periods, such fCO₂ increase is not always observed. In a recent study focused in the mid-latitude NA (40-50°N), Macovei et al. (2019) showed that fCO₂ is highly variable with a small trend of +0.37 (\pm 0.22) µatm yr⁻¹ in 2002-2016 implying a significant increase of the CO₂ uptake in this region especially after 2010 when we also observed a sudden drop of fCO₂ in summer in the NASPG (Fig. 4g,h). Our results added to those from Macovei et al. (2019) suggest the ocean CO₂ sink increased in the North Atlantic (north of 40°N) at least since 2007 and until 2017, contributing to the increase of the global ocean CO₂ sink (Friedlingstein et al., 2019). At the NA basin
- 20 scale this is consistent with results deduced from fCO_2 reconstructed data-based methods (Denvil-Sommer et al., 2019; Gregor et al., 2019) but opposed to the ocean CO_2 sink variability generated by current ESM models implying uncertainties to predict the evolution of the NA CO_2 sink in the future (Lebehot et al., 2019).

For pH the long-term trend in the NASPG of -0.0017 yr⁻¹ is in the range of what is observed in other oceanic regions but we note some differences.
This trend is equal to the trend estimated at BATS station but is lower than in the Irminger Sea and higher than in the Iceland Sea (Bates et al., 2014). It is also lower than the pH trend of -0.0020 yr⁻¹ estimated in the North Atlantic Subpolar region in 1991-2011 (Lauvset et al., 2015) and -0.0024 yr⁻¹ recently observed in the NA waters in the North Sea in 2004-2015 (Omar et al., 2019).

<u>Given the large differences of fCO₂ and pH trends at regional scale as listed above, our results among many others highlight the need for</u>
 sustained ocean carbonates system time-series observation in different regions and if possible over long period as it has been strongly recommended at the recent Ocean-Obs19 conference (Tilbrook et al., 2019; Wanninkhof et al., 2019).

An understanding of these differences also calls for a comprehensive analysis including a synthesis of all DIC and TA sea surface observations collected in different regions. This should be achieved at an international level as is done for sea surface fCO₂ in the frame of SOCAT (Bakker

35 et al., 2016) or for CLIVAR/GO-SHIP cruises assembled in GLODAP (Olsen et al., 2019). In addition to ship-based observations, the analysis of data from BGC-Argo floats equipped with pH sensors (together with temperature and salinity sensors, from which TA, DIC and fCO₂ can be estimated, e.g. Williams et al., 2017) will help to better constrain spatial, seasonal and inter-annual variability. Such data synthesis would also help to validate ocean and earth system models that at present do not represent correctly the temporal change of marine biogeochemistry as demonstrated by Lebehot et al. (2019) for the North Atlantic.

40

Data availability. The data set is freely available and is accessible at http://www.seanoe.org/data/00434/54517/ (http://doi.org/10.17882/54517, Reverdin et al. (2018b).

Author contributions. CL produced the data analyses and wrote the manuscript with inputs from CLMNM, GR and NMCLM. GR, NM and VR produced the data synthesis. SO provided the nutrients data. JF provided the DIC and TA data.

5 *Competing interests.* The authors declare that they have no conflict of interest.

Acknowledgments. The SURATLANT project is supported by the French institute INSU (Institut National des Sciences de l'Univers), the Lamont-Doherty Earth Observatory (LDEO), the National Oceanic and Atmospheric Administration (NOAA) - Atlantic Oceanographic and Meteorological Laboratory (AOML) and the Climate Program Office (CPO). We thank the EIMSKIP Company and the MFRI team, both based

10 in Reykjavik (Iceland), for their cooperation in sea water sampling and analysis. We also thank the numerous scientific volunteers who worked at sea, as well as the crew and captain of the vessels for their help. We thank the reviewers, Are Olsen and an anonymous reviewer for their helpful comments on this work. We have an emotional thought for our late colleague Taro Takahashi who contributed to initiate this sampling in 1993 and was a strong source of motivation for maintaining this long time monitoring.

References

- Bakker, D. C. E., Pfeil, B., Landa, C. S., Metzl, N., O'Brien, K. M., Olsen, A., Smith, K., Cosca, C., Harasawa, S., Jones, S. D., Nakaoka, S., Nojiri, Y., Schuster, U., Steinhoff, T., Sweeney, C., Takahashi, T., Tilbrook, B., Wada, C., Wanninkhof, R., Alin, S. R., Balestrini, C. F., Barbero, L., Bates, N. R., Bianchi, A. A., Bonou, F., Boutin, J., Bozec, Y., Burger, E. F., Cai, W.-J., Castle, R. D., Chen, L., Chierici, M., Currie, K., Evans, W., Featherstone, C., Feely, R. A., Fransson, A., Goyet, C., Greenwood, N., Gregor, L., Hankin, S., Hardman-Mountford, N. J., Harlay, J., Hauck, J., Hoppema, M., Humphreys, M. P., Hunt, C. W., Huss, B., Ibánhez, J. S. P., Johannessen, T., Keeling, R., Kitidis, V., Körtzinger, A., Krasakopoulou, E. Kuwata, A., Landschützer, P., Lauvset, S. K., Lafavre, N., Monaco, C. L., Manka, A., Mathis, I. T., Marlivat, S., Kortzinger, N., Kortzinger, S. K., Lafavre, N., Monaco, C. L., Manka, A., Mathis, I. T., Marlivat, A., Krasakopoulou, E., Kuwata, A., Landschützer, P., Lauvset, S. K., Lafavre, N., Monaco, C. L., Manka, A., Mathis, I. T., Marlivat, A., Krasakopoulou, E., Kuwata, A., Landschützer, P., Lauvset, S. K., Lafavre, N., Monaco, C. L., Manka, A., Mathis, J. T., Marlivat, A., Krasakopoulou, E., Kuwata, A., Landschützer, P., Lauvset, S. K., Lafavre, N., Monaco, C. J., Manka, A., Mathis, J. T., Marlivat, M., Kumata, A., Kataka, K., Kuwata, A., Landschützer, P., Lauvset, S. K., Lafavre, N., Monaco, C. L., Manka, A., Mathis, J. T., Marlivat, A., Kataka, M., Kumata, A., Landschützer, P., Lauvset, S. K., Lafavre, N., Monaco, C. L., Manka, A., Mathis, J., Marlivat, M., Kumata, A., Kataka, Mathis, J. T., Marlivat, A., Kataka, Kataka, Kataka, A., Kataka, A., Kataka, K
- A., Kozyr, A., Krasakopoulou, E., Kuwata, A., Landschützer, P., Lauvset, S. K., Lefèvre, N., Monaco, C. L., Manke, A., Mathis, J. T., Merlivat, L., Millero, F. J., Monteiro, P. M. S., Munro, D. R., Murata, A., Newberger, T., Omar, A. M., Ono, T., Paterson, K., Pearce, D., Pierrot, D., Robbins, L. L., Saito, S., Salisbury, J., Schlitzer, R., Schneider, B., Schweitzer, R., Sieger, R., Skjelvan, I., Sullivan, K. F., Sutherland, S. C., Sutton, A. J., Tadokoro, K., Telszewski, M., Tuma, M., Heuven, S. M. A. C. van, Vandemark, D., Ward, B., Watson, A. J. and Xu, S.: A multidecade record of high-quality fCO2 data in version 3 of the Surface Ocean CO2 Atlas (SOCAT), Earth System Science Data, 8(2), 383–413, doi:https://doi.org/10.5194/essd-8-383-2016, 2016.

Bates, N., Astor, Y., Church, M., Currie, K., Dore, J., Gonaález-Dávila, M., Lorenzoni, L., Muller-Karger, F., Olafsson, J. and Santa-Casiano, M.: A Time-Series View of Changing Ocean Chemistry Due to Ocean Uptake of Anthropogenic CO2 and Ocean Acidification, Oceanography, 27(1), 126–141, doi:10.5670/oceanog.2014.16, 2014.

Beaugrand, G., McQuatters-Gollop, A., Edwards, M. and Goberville, E.: Long-term responses of North Atlantic calcifying plankton to climate
 change, Nature Clim Change, 3(3), 263–267, doi:10.1038/nclimate1753, 2013.

Becker, M., Steinhoff, T. and Körtzinger, A.: A Detailed View on the Seasonality of Stable Carbon Isotopes Across the North Atlantic, Global Biogeochemical Cycles, 32(9), 1406–1419, doi:10.1029/2018GB005905, 2018.

Breeden, M. L. and McKinley, G. A.: Climate impacts on multidecadal pCO2 variability in the North Atlantic: 1948–2009, Biogeosciences, 13(11), 3387–3396, doi:10.5194/bg-13-3387-2016, 2016.

35 Brown, C. W. and Yoder, J. A.: Distribution pattern of coccolithophorid blooms in the western North Atlantic Ocean, Continental Shelf Research, 14(2), 175–197, doi:10.1016/0278-4343(94)90012-4, 1994.

Chafik, L., Rossby, T. and Schrum, C.: On the spatial structure and temporal variability of poleward transport between Scotland and Greenland, Journal of Geophysical Research: Oceans, 119(2), 824–841, doi:10.1002/2013JC009287, 2014.

Chafik, L., Nilsen, J. E. Ø., Dangendorf, S., Reverdin, G. and Frederikse, T.: North Atlantic Ocean Circulation and Decadal Sea Level Change
 During the Altimetry Era, Scientific Reports, 9(1), 1–9, doi:10.1038/s41598-018-37603-6, 2019.

Clement, D. and Gruber, N.: The eMLR(C*) Method to Determine Decadal Changes in the Global Ocean Storage of Anthropogenic CO2, Global Biogeochemical Cycles, 32(4), 654–679, doi:10.1002/2017GB005819, 2018.

Corbière, A., Metzl, N., Reverdin, G., Brunet, C. and Takahashi, T.: Interannual and decadal variability of the oceanic carbon sink in the North Atlantic subpolar gyre, Tellus B, 59(2), 168–178, doi:10.1111/j.1600-0889.2006.00232.x, 2007.

De Boisséson, E., Thierry, V., Mercier, H., Caniaux, G. and Desbruyères, D.: Origin, formation and variability of the Subpolar Mode Water located over the Reykjanes Ridge, Journal of Geophysical Research: Oceans, 117(C12), doi:10.1029/2011JC007519, 2012.

5 Denvil-Sommer, A., Gehlen, M., Vrac, M. and Mejia, C.: LSCE-FFNN-v1: a two-step neural network model for the reconstruction of surface ocean pCO2 over the global ocean, Geoscientific Model Development, 12(5), 2091–2105, doi:https://doi.org/10.5194/gmd-12-2091-2019, 2019.

Desbruyères, D., Mercier, H. and Thierry, V.: On the mechanisms behind decadal heat content changes in the eastern subpolar gyre, Progress in Oceanography, 132, 262–272, doi:10.1016/j.pocean.2014.02.005, 2015.

Dickson, A. G.: Thermodynamics of the dissociation of boric acid in synthetic seawater from 273.15 to 318.15 K, Deep Sea Research Part A. Oceanographic Research Papers, 37(5), 755–766, doi:10.1016/0198-0149(90)90004-F, 1990.

Dickson, A. G. and Millero, F. J.: A comparison of the equilibrium constants for the dissociation of carbonic acid in seawater media, Deep Sea Research Part A, Oceanographic Research Papers, 34(10), 1733–1743, doi:10.1016/0198-0149(87)90021-5, 1987.

Dlugokencky, E. J., Lang, P. M., Mund, J. W., Crotwell, M. J. and Thoning, K. W.: Atmospheric Carbon Dioxide Dry Air Mole Fractions from the NOAA ESRL Carbon Cycle Cooperative Global Air Sampling Network, 1968-2017, Version: 2018-07-31,Path:
 15 ftp://aftp.cmdl.noaa.gov/data/trace gases/co2/flask/surface/., 2018.

Doney, S., Bopp, L. and Long, M.: Historical and Future Trends in Ocean Climate and Biogeochemistry, oceanog, 27(1), 108–119, doi:10.5670/oceanog.2014.14, 2014.

Doney, S. C., Fabry, V. J., Feely, R. A. and Kleypas, J. A.: Ocean Acidification: The Other CO2 Problem, Annual Review of Marine Science, 1(1), 169–192, doi:10.1146/annurev.marine.010908.163834, 2009.

20 Fay, A. R. and McKinley, G. A.: Global trends in surface ocean pCO2 from in situ data, Global Biogeochemical Cycles, 27(2), 541–557, doi:10.1002/gbc.20051, 2013.

Fay, A. R. and McKinley, G. A.: Global open-ocean biomes: mean and temporal variability, Earth System Science Data, 6(2), 273-284, doi:https://doi.org/10.5194/essd-6-273-2014, 2014.

- Friedlingstein, P., Jones, M. W., O'Sullivan, M., Andrew, R. M., Hauck, J., Peters, G. P., Peters, W., Pongratz, J., Sitch, S., Quéré, C. L., Bakker,
 D. C. E., Canadell, J. G., Ciais, P., Jackson, R. B., Anthoni, P., Barbero, L., Bastos, A., Bastrikov, V., Becker, M., Bopp, L., Buitenhuis, E., Chandra, N., Chevallier, F., Chini, L. P., Currie, K. I., Feely, R. A., Gehlen, M., Gilfillan, D., Gkritzalis, T., Goll, D. S., Gruber, N., Gutekunst, S., Harris, I., Haverd, V., Houghton, R. A., Hurtt, G., Ilyina, T., Jain, A. K., Joetzjer, E., Kaplan, J. O., Kato, E., Klein Goldewijk, K., Korsbakken, J. I., Landschützer, P., Lauvset, S. K., Lefèvre, N., Lenton, A., Lienert, S., Lombardozzi, D., Marland, G., McGuire, P. C., Melton, J. R., Metzl, N., Munro, D. R., Nabel, J. E. M. S., Nakaoka, S.-I., Neill, C., Omar, A. M., Ono, T., Peregon, A., Pierrot, D., Poulter, B., Rehder, G., Resplandy, L., Robertson, E., Rödenbeck, C., Séférian, R., Schwinger, J., Smith, N., Tans, P. P., Tian, H., Tilbrook, B., Tubiello, F. N., Werf, G. R. van
- 30 L., Robertson, E., Rodenbeck, C., Seferian, R., Schwinger, J., Smith, N., Tans, P. P., Tian, H., Tibrook, B., Tubiello, F. N., Wert, G. R. van der, Wiltshire, A. J. and Zaehle, S.: Global Carbon Budget 2019, Earth System Science Data, 11(4), 1783–1838, doi:https://doi.org/10.5194/essd-11-1783-2019, 2019.

Friis, K., Körtzinger, A. and Wallace, D. W. R.: The salinity normalization of marine inorganic carbon chemistry data, Geophysical Research Letters, 30(2), doi:10.1029/2002GL015898, 2003.

35 Fröb, F., Olsen, A., Våge, K., Moore, G. W. K., Yashayaev, I., Jeansson, E. and Rajasakaren, B.: Irminger Sea deep convection injects oxygen and anthropogenic carbon to the ocean interior, Nat Commun, 7(1), 1–8, doi:10.1038/ncomms13244, 2016.

Fröb, F., Olsen, A., Pérez, F. F., García-Ibáñez, M. I., Jeansson, E., Omar, A. and Lauvset, S. K.: Inorganic carbon and water masses in the Irminger Sea since 1991, Biogeosciences, 15(1), 51–72, doi:https://doi.org/10.5194/bg-15-51-2018, 2018.

Gruber, N., Landschützer, P. and Lovenduski, N. S.: The Variable Southern Ocean Carbon Sink, Annual Review of Marine Science, 11(1), 159–
 40 186, doi:10.1146/annurev_marine_121916_063407, 2019.

Fröb, F., Olsen, A., Becker, M., Chafik, L., Johannessen, T., Reverdin, G. and Omar, A.: Wintertime fCO2 Variability in the Subpolar North Atlantic Since 2004, Geophysical Research Letters, 46(3), 1580–1590, doi:10.1029/2018GL080554, 2019.

García-Ibáñez, M. I., Zunino, P., Fröb, F., Carracedo, L. I., Ríos, A. F., Mercier, H., Olsen, A. and Pérez, F. F.: Ocean acidification in the subpolar North Atlantic: rates and mechanisms controlling pH changes, Biogeosciences, 13(12), 3701–3715, doi:https://doi.org/10.5194/bg-13-3701-2016, 2016.

Gregor, L., Lebehot, A. D., Kok, S., Monteiro, S. and M, P.: A comparative assessment of the uncertainties of global surface ocean CO2 estimates
 using a machine-learning ensemble (CSIR-ML6 version 2019a) – have we hit the wall?, Geoscientific Model Development, 12(12), 5113–5136, doi:https://doi.org/10.5194/gmd-12-5113-2019, 2019.

Gruber, N., Clement, D., Carter, B. R., Feely, R. A., Heuven, S. van, Hoppema, M., Ishii, M., Key, R. M., Kozyr, A., Lauvset, S. K., Lo Monaco, C., Mathis, J. T., Murata, A., Olsen, A., Perez, F. F., Sabine, C. L., Tanhua, T. and Wanninkhof, R.: The oceanic sink for anthropogenic CO2 from 1994 to 2007, Science, 363(6432), 1193–1199, doi:10.1126/science.aau5153, 2019a.

10 Gruber, N., Clement, D., Carter, B. R., Feely, R. A., Heuven, S. van, Hoppema, M., Ishii, M., Key, R. M., Kozyr, A., Lauvset, S. K., Lo Monaco, C., Mathis, J. T., Murata, A., Olsen, A., Perez, F. F., Sabine, C. L., Tanhua, T. and Wanninkhof, R.: The oceanic sink for anthropogenic CO2 from 1994 to 2007 - the data (NCEI Accession 0186034). NOAA National Centers for Environmental Information. Dataset. https://doi.org/10.25921/wdn2-pt10, 2019b, [acces 17/06/2019].

Häkkinen, S. and Rhines, P. B.: Decline of Subpolar North Atlantic Circulation During the 1990s, Science, 304(5670), 555–559, doi:10.1126/science.1094917, 2004.

Häkkinen, S. and Rhines, P. B.: Shifting surface currents in the northern North Atlantic Ocean, Journal of Geophysical Research: Oceans, 114(C4), doi:10.1029/2008JC004883, 2009.

Häkkinen, S., Rhines, P. B. and Worthen, D. L.: Atmospheric Blocking and Atlantic Multidecadal Ocean Variability, Science, 334(6056), 655–659, doi:10.1126/science.1205683, 2011.

20 Häkkinen, S., Rhines, P. B. and Worthen, D. L.: Northern North Atlantic sea surface height and ocean heat content variability, Journal of Geophysical Research: Oceans, 118(7), 3670–3678, doi:10.1002/jgrc.20268, 2013.

Hartmann, D.L., A.M.G. Klein Tank, M. Rusticucci, L.V. Alexander, S. Brönnimann, Y. Charabi, F.J. Dentener, E.J. Dlugokencky, D.R. Easterling, A. Kaplan, B.J. Soden, P.W. Thorne, M. Wild and P.M. Zhai.: Observations: Atmosphere and Surface. In: Climate Change 2013: The Physical Science Basis. Contribution of Working Group I to the Fifth Assessment Report of the Intergovernmental Panel on Climate Change 1999. The Physical Science Basis. Contribution of Working Group I to the Fifth Assessment Report of the Intergovernmental Panel on Climate Change 1999. The Physical Science Basis. Contribution of Working Group I to the Fifth Assessment Report of the Intergovernmental Panel on Climate Change 1999. The Physical Science Basis Contribution of Working Contribution of Wor

25 [Stocker, T.F., D. Qin, G.-K. Plattner, M. Tignor, S.K. Allen, J. Boschung, A. Nauels, Y. Xia, V. Bex and P.M. Midgley (eds.)]. Cambridge University Press, Cambridge, United Kingdom and New York, NY, USA, pp. 159–254, doi:10.1017/CBO9781107415324.008, 2013.

Jones, P. D., Jonsson, T. and Wheeler, D. A.: Monthly values of the North Atlantic Oscillation Index from 1821 to 2000, Supplement to: Jones, PD et al. (1997): Extension to the North Atlantic Oscillation using early instrumental pressure observations from Gibraltar and South West
 30 Iceland. International Journal of Climatology, 17(13), 1433-1450, https://doi.org/10.1002/(SICI)1097-0088(19971115)17:13%3C1433::AID-JOC203%3E3.0.CO;2 P, doi:https://doi.org/10.1594/PANGAEA.56559, 1997.

Josey, S. A., Somot, S. and Tsimplis, M.: Impacts of atmospheric modes of variability on Mediterranean Sea surface heat exchange, Journal of Geophysical Research: Oceans, 116(C2), doi:10.1029/2010JC006685, 2011.

 Hátún, H., Azetsu-Scott, K., Somavilla, R., Rey, F., Johnson, C., Mathis, M., Mikolajewicz, U., Coupel, P., Tremblay, J.-É., Hartman, S., Pacariz,
 S. V., Salter, I. and Ólafsson, J.: The subpolar gyre regulates silicate concentrations in the North Atlantic, Sci Rep, 7(1), 1–9, doi:10.1038/s41598-017-14837-4, 2017.

van Heuven, S., Pierrot, D., Rae, J. W. B., Lewis, E. and Wallace, D. W. R.: MATLAB Program Developed for CO2 System Calculations. ORNL/CDIAC-105b., doi:https://doi.org/10.3334/cdiac/otg.co2sys_matlab_v1.1, 2011.

 Holliday, N. P., Bersch, M., Berx, B., Chafik, L., Cunningham, S., Florindo-Lopez, C., Hátún, H., Johns, W., Josey, S., A., Larsen, K., M., H.,
 Mulet, S., Oltmanns, M., Reverdin, G., Rossby, T., Thierry, V., Valdimarsson, H.: Ocean Circulation Changes Cause The Largest Freshening Event For 120 Years In The Eastern Subpolar North Atlantic, NCOMMS-19-10051C accepted paper, 2019.

Jiang, L.-Q., Carter, B. R., Feely, R. A., Lauvset, S. K. and Olsen, A.: Surface ocean pH and buffer capacity: past, present and future, Sci Rep, 9(1), 1–11, doi:10.1038/s41598-019-55039-4, 2019.

de Jong, M. F. and de Steur, L.: Strong winter cooling over the Irminger Sea in winter 2014–2015, exceptional deep convection, and the
 emergence of anomalously low SST, Geophysical Research Letters, 43(13), 7106–7113, doi:10.1002/2016GL069596, 2016.

Josey, S. A., Hirschi, J. J.-M., Sinha, B., Duchez, A., Grist, J. P. and Marsh, R.: The Recent Atlantic Cold Anomaly: Causes, Consequences, and Related Phenomena, Annual Review of Marine Science, 10(1), 475–501, doi:10.1146/annurev-marine-121916-063102, 2018.

Keller, K., Joos, F., Raible, C., Cocco, V., Frolicher, T., Dunne, J., Gehlen, M., Bopp, L., Orr, J., Tjiputra, J., Heinze, C., Segscheider, J., Roy, T. and Metzl, N.: Variability of the Ocean Carbon Cycle in Response to the North Atlantic Oscillation, Tellus B, 64, 18738, doi: https://doi.org/10.3402/tellusb.v64i0.18738, 2012.

5

Key, R. M., Olsen, A., van Heuven, S., Lauvset, S. K., Velo, A., Lin, X., Schirnick, C., Kozyr, A., Tanhua, T., Hoppema, M., Jutterström, S., Steinfeldt, R., Jeansson, E., Ishii, M., Perez, F. F. and Suzuki, T.: Global Ocean Data Analysis Project, Version 2 (GLODAPv2), ORNL/CDIAC-162, NDP-093, doi:10.3334/CDIAC/OTG. NDP093 GLODAPv2, 2015.

Khatiwala, S., Tanhua, T., Mikaloff Fletcher, S., Gerber, M., Doney, S. C., Graven, H. D., Gruber, N., McKinley, G. A., Murata, A., Ríos, A. F.
and Sabine, C. L.: Global ocean storage of anthropogenic carbon, Biogeosciences, 10(4), 2169–2191, doi:https://doi.org/10.5194/bg-10-2169-2013, 2013.

Kwiatkowski, L. and Orr, J. C.: Diverging seasonal extremes for ocean acidification during the twenty-first century, Nature Clim Change, 8(2), 141–145, doi:10.1038/s41558-017-0054-0, 2018.

 Landschützer, P., Gruber, N., Bakker, D. C. E., Schuster, U., Nakaoka, S., Payne, M. R., Sasse, T. P. and Zeng, J.: A neural network-based
 estimate of the seasonal to inter-annual variability of the Atlantic Ocean carbon sink, <u>-23Biogeosciences</u>, 10, 7793–7815, doi:doi:10.5194/bg-<u>10-7793-2013</u>, 2013.

Landschützer, P., Gruber, N., Bakker, D. C. E., Stemmler, I. and Six, K. D.: Strengthening seasonal marine CO2 variations due to increasing atmospheric CO2, Nature Clim Change, 8(2), 146–150, doi:10.1038/s41558-017-0057-x, 2018.

Landschützer, P., Ilyina, T. and Lovenduski, N. S.: Detecting Regional Modes of Variability in Observation-Based Surface Ocean pCO2, Geophysical Research Letters, 0(0), doi:10.1029/2018GL081756, 2019.

Lauvset, S. K. and Gruber, N.: Long-term trends in surface ocean pH in the North Atlantic, 0304-4203, doi:10.1016/j.marchem.2014.03.009, 2014.

Lauvset, S. K., Gruber, N., Landschützer, P., Olsen, A. and Tjiputra, J.: Trends and drivers in global surface ocean pH over the past 3 decades, Biogeosciences, 12(5), 1285–1298, doi:10.5194/bg-12-1285-2015, 2015.

- Le Quéré, C., Andrew, R. M., Friedlingstein, P., Sitch, S., Hauck, J., Pongratz, J., Pickers, P. A., Korsbakken, J. I., Peters, G. P., Canadell, J. G., Arneth, A., Arora, V. K., Barbero, L., Bastos, A., Bopp, L., Chevallier, F., Chini, L. P., Ciais, P., Doney, S. C., Gkritzalis, T., Goll, D. S., Harris, I., Haverd, V., Hoffman, F. M., Hoppema, M., Houghton, R. A., Hurtt, G., Ilyina, T., Jain, A. K., Johannessen, T., Jones, C. D., Kato, E., Keeling, R. F., Goldewijk, K. K., Landschützer, P., Lefèvre, N., Lienert, S., Liu, Z., Lombardozzi, D., Metzl, N., Munro, D. R., Nabel, J. E. M. S., Nakaoka, S., Neill, C., Olsen, A., Ono, T., Patra, P., Peregon, A., Peters, W., Peylin, P., Pfeil, B., Pierrot, D., Poulter, B., Rehder, G., Resplandy, L., Robertson, E., Rocher, M., Rödenbeck, C., Schuster, U., Schwinger, J., Séférian, R., Skjelvan, I., Steinhoff, T., Sutton, A., Tans, P. P., Tian,
- 30 L., Robertson, E., Rocher, M., Rödenbeck, C., Schuster, U., Schwinger, J., Séférian, R., Skjelvan, I., Steinhoff, T., Sutton, A., Tans, P. P., Tian, H., Tilbrook, B., Tubiello, F. N., Laan-Luijkx, I. T. van der, Werf, G. R. van der, Viovy, N., Walker, A. P., Wiltshire, A. J., Wright, R., Zaehle, S. and Zheng, B.: Global Carbon Budget 2018, Earth System Science Data, 10(4), 2141–2194, doi:https://doi.org/10.5194/essd-10-2141-2018, 2018.
- Lebehot, A. D., Halloran, P. R., Watson, A. J., McNeall, D., Ford, D. A., Landschützer, P., Lauvset, S. K. and Schuster, U.: Reconciling
 Observation and Model Trends in North Atlantic Surface CO2, Global Biogeochemical Cycles, 0(0), doi:10.1029/2019GB006186, 2019.

Lee, K., Tong, L. T., Millero, F. J., Sabine, C. L., Dickson, A. G., Goyet, C., Park, G.-H., Wanninkhof, R., Feely, R. A. and Key, R. M.: Global relationships of total alkalinity with salinity and temperature in surface waters of the world's oceans, Geophysical Research Letters, 33(19), doi:10.1029/2006GL027207, 2006.

Lewis, E., Wallace, D. and Allison, L. J.: Program developed for <u>CO2CO{sub 2}</u> system calculations, Brookhaven National Lab., Dept. of 40 Applied Science, Upton, NY (United States); Oak Ridge National Lab., Carbon Dioxide Information Analysis Center, TN (United States)., 1998.

Loveday, B. R. and Smyth, T.: A 40-year global data set of visible-channel remote-sensing reflectances and coccolithophore bloom occurrence derived from the Advanced Very High Resolution Radiometer catalogue, Earth System Science Data, 10(4), 2043–2054, doi:https://doi.org/10.5194/essd-10-2043-2018, 2018.

Macovei, V. A., Hartman, S. E., Schuster, U., Torres-Valdés, S., Moore, C. M. and Sanders, R. J.: Impact of physical and biological processes
 on temporal variations of the ocean carbon sink in the mid-latitude North Atlantic (2002-2016), Progress in Oceanography, 102223, doi:10.1016/j.pocean.2019.102223, 2019.

McKinley, G. A., Fay, A. R., Takahashi, T. and Metzl, N.: Convergence of atmospheric and North Atlantic carbon dioxide trends on multidecadal timescales, Nature Geoscience, 4(9), 606–610, doi:10.1038/ngeo1193, 2011.

McKinley, G. A., Ritzer, A. L. and Lovenduski, N. S.: Mechanisms of northern North Atlantic biomass variability, Biogeosciences, 15(20), 6049–6066, doi:https://doi.org/10.5194/bg-15-6049-2018, 2018.

5 Mehrbach, C., Culberson, C. H., Hawley, J. E. and Pytkowicx, R. M.: Measurement of the Apparent Dissociation Constants of Carbonic Acid in Seawater at Atmospheric Pressure1, Limnology and Oceanography, 18(6), 897–907, doi:10.4319/lo.1973.18.6.0897, 1973.

Metzl, N., Corbière, A., Reverdin, G., Lenton, A., Takahashi, T., Olsen, A., Johannessen, T., Pierrot, D., Wanninkhof, R., Ólafsdóttir, S. R., Olafsson, J. and Ramonet, M.: Recent acceleration of the sea surface fCO2 growth rate in the North Atlantic subpolar gyre (1993–2008) revealed by winter observations, Global Biogeochemical Cycles, 24(4), doi:10.1029/2009GB003658, 2010.

- 10 Metzl, N., Ferron, B., Lherminier, P., Sarthou, G., Thierry, V.: Discrete profile measurements of dissolved inorganic carbon (DIC), total alkalinity (TALK), temperature and salinity during the multiple ships Observatoire de la variabilité interannuelle et décennale en Atlantique Nord (OVIDE) project, OVIDE-2006, OVIDE-2008, OVIDE-2010, OVIDE-2012, OVIDE-2014 cruises in the North Atlantic Ocean from 2006-05-23 to 2014-06-30 (NCEI Accession 0177219). Version 1.1. NOAA National Centers for Environmental Information. Dataset. doi:10.25921/v0qt-ms48, 2018 [acces 29/11/2019].
- 15 Millero, F. J., Lee, K. and Roche, M.: Distribution of alkalinity in the surface waters of the major oceans, Marine Chemistry, 60(1), 111–130, doi:10.1016/S0304-4203(97)00084-4, 1998.

Millero, F. J., Feistel, R., Wright, D. G., and McDougall, T. J.: The composition of standar seawater and the definition of the referencecomposition salinity scale. Deep Sea Research Part I: Oceanographic Research Papers, 55(1), 50-72, doi: https://doi.org/10.1016/j.dsr.2007.10.001, 2008.

20 Nigam, S., Ruiz-Barradas, A. and Chafik, L.: Gulf Stream Excursions and Sectional Detachments Generate the Decadal Pulses in the Atlantic Multidecadal Oscillation, Journal of Climate, 31(7), 2853–2870, doi:10.1175/JCLI-D-17-0010.1, 2018.

Olafsson, J., Olafsdottir, S. R., Benoit-Cattin, A., Danielsen, M. and Takahashi, T.: North Atlantic Ocean acidification from time series measurements, IOP Conf. Ser.: Earth Environ. Sci., 6(46), 462005, doi:10.1088/1755-1307/6/46/462005, 2009.

Ólafsson, J., Ólafsdóttir, S. R., Benoit-Cattin, A. and Takahashi, T.: Hydrochemistry measured on water bottle samples during Bjarni
 Saemundsson cruise B11/2004, In supplement to: Ólafsson, J et al. (2010): The Irminger Sea and the Iceland Sea time series measurements of sea water carbon and nutrient chemistry 1983–2006. Earth System Science Data, 2(1), 99-104, https://doi.org/10.5194/essd-2-99-2010, doi:https://doi.org/10.1594/PANGAEA.774097, 2010.

World Meteorological Olsen, A., Key, R. M., Heuven, S. van, Lauvset, S. K., Velo, A., Lin, X., Schirnick, C., Kozyr, A., Tanhua, T., Hoppema, M., Jutterström, S., Steinfeldt, R., Jeansson, E., Ishii, M., Pérez, F. F. and Suzuki, T.: The Global Ocean Data Analysis Project version 2
 (GLODAPv2) – an internally consistent data product for the world ocean, Earth System Science Data, 8(2), 297–323, doi:https://doi.org/10.5194/essd-8-297-2016, 2016.

Olsen, A., Lange, N., Key, R. M., Tanhua, T., Álvarez, M., Becker, S., Bittig, H. C., Carter, B. R., Cotrim da Cunha, L., Feely, R. A., Heuven, S. van, Hoppema, M., Ishii, M., Jeansson, E., Jones, S. D., Jutterström, S., Karlsen, M. K., Kozyr, A., Lauvset, S. K., Monaco, C. L., Murata, A., Pérez, F. F., Pfeil, B., Schirnick, C., Steinfeldt, R., Suzuki, T., Telszewski, M., Tilbrook, B., Velo, A. and Wanninkhof, R.: GLODAPv2.2019 – an update of GLODAPv2, Earth System Science Data, 11(3), 1437–1461, doi:https://doi.org/10.5194/essd-11-1437-2019, 2019.

35

Omar, A. M., Thomas, H., Olsen, A., Becker, M., Skjelvan, I. and Reverdin, G.: Trends of Ocean Acidification and pCO2 in the Northern North Sea, 2003–2015, Journal of Geophysical Research: Biogeosciences, 124(10), 3088–3103, doi:10.1029/2018JG004992, 2019.

Ono, H., Kosugi, N., Toyama, K., Tsujino, H., Kojima, A., Enyo, K., Iida, Y., Nakano, T. and Ishii, M.: Acceleration of Ocean Acidification in the Western North Pacific, Geophysical Research Letters, (46), doi:10.1029/2019GL085121, 2019.

- 40 Organization (WMO), W. M., (UNESCO) United Nations Educational, S. and C. O., Commission, (IOC) Intergovernmental Oceanographic, Programme, (UNEP) United Nations Environment, Science, (ICSU) International Council for, Climate (OOPC-21), 21st Session of the Ocean Observations Panel for and World Meteorological Organization (WMO): GCOS, 217. 21st Session of the Ocean Observations Panel for Climate (the GOOS Physics and Climate Panel) (OOPC-21), WMO., 2018.
- Pierrot, D. E., Wallace, D. W. R. and Lewis, E.: MS Excel Program Developed for CO2 System Calculations, Carbon Dioxide Information
 45 Analysis Center, Oak Ridge National Laboratory, U.S. Department of Energy, Oak Ridge, Tennessee, doi:10.3334/CDIAC/otg.CO2SYS_XLS_CDIAC105a, 2006.

Reverdin, G.: North Atlantic Subpolar Gyre Surface Variability (1895–2009), J. Climate, 23(17), 4571–4584, doi:10.1175/2010JCLI3493.1, 2010.

Orr, J. C., Fabry, V. J., Aumont, O., Bopp, L., Doney, S. C., Feely, R. A., Gnanadesikan, A., Gruber, N., Ishida, A., Joos, F., Key, R. M., Lindsay, K., Maier-Reimer, E., Matear, R., Monfray, P., Mouchet, A., Najjar, R. G., Plattner, G.-K., Rodgers, K. B., Sabine, C. L., Sarmiento,
J. L., Schlitzer, R., Slater, R. D., Totterdell, I. J., Weirig, M.-F., Yamanaka, Y. and Yool, A.: Anthropogenic ocean acidification over the twentyfirst century and its impact on calcifying organisms, Nature, 437(7059), 681–686, doi:10.1038/nature04095, 2005.

Orr, J. C., Epitalon, J.-M., Dickson, A. G. and Gattuso, J.-P.: Routine uncertainty propagation for the marine carbon dioxide system, Marine Chemistry, 207, 84–107, doi:10.1016/j.marchem.2018.10.006, 2018.

Pickart, R. S., Spall, M. A., Ribergaard, M. H., Moore, G. W. K. and Milliff, R. F.: Deep convection in the Irminger Sea forced by the Greenland
 tip jet, Nature, 424(6945), 152–156, doi:10.1038/nature01729, 2003.

Piron, A., Thierry, V., Mercier, H. and Caniaux, G.: Gyre-scale deep convection in the subpolar North Atlantic Ocean during winter 2014–2015, Geophysical Research Letters, 44(3), 1439–1447, doi:10.1002/2016GL071895, 2017.

Racapé, V., Pierre, C., Metzl, N., Lo Monaco, C., Reverdin, G., Olsen, A., Morin, P., Vázquez-Rodríguez, M., Ríos, A. F. and Pérez, F. F.: <u>Anthropogenic carbon changes in the Irminger Basin (1981–2006): Coupling δ13CDIC and DIC observations, Journal of Marine Systems, 126,</u> 24–32, doi:10.1016/j.jmarsys.2012.12.005, 2013.

Racapé, V., Metzl, N., Pierre, C., Reverdin, G., Quay, P. D. and Olafsdottir, S. R.: The seasonal cycle of delta 13C DIC in the North Atlantic subpolar gyre, Biogeosciences, 11(6), 1683–1692, doi:10.5194/bg-11-1683-2014, 2014.

Reverdin, G., Valdimarsson, H., Alory, G., Diverres, D., Bringas, F., Goni, G., Heilmann, L., Chafik, L., Szekely, T. and Friedman, A. R.: North Atlantic subpolar gyre along predetermined ship tracks since 1993: a monthly data set of surface temperature, salinity, and density, Earth System Science Data, 10(3), 1403–1415, doi:https://doi.org/10.5194/essd-10-1403-2018, 2018a.

Reverdin, G., Metzl, N., Olafsdottir, S., Racapé, V., Takahashi, T., Benetti, M., Valdimarsson, H., Benoit-Cattin, A., Danielsen, M., Fin, J., Naamar, A., Pierrot, D., Sullivan, K., Bringas, F. and Goni, G.: SURATLANT: a 1993–2017 surface sampling in the central part of the North Atlantic subpolar gyre, Earth System Science Data, 10(4), 1901–1924, doi:10.5194/essd-10-1901-2018, 2018b.

Robson, J., Sutton, R., Lohmann, K., Smith, D. and Palmer, M. D.: Causes of the Rapid Warming of the North Atlantic Ocean in the Mid-1990s,
 J. Climate, 25(12), 4116–4134, doi:10.1175/JCLI D 11-00443.1, 2012.

Rivero-Calle, S., Gnanadesikan, A., Del Castillo, C. E., Balch, W. M. and Guikema, S. D.: Multidecadal increase in North Atlantic coccolithophores and the potential role of rising CO2, Science, 350(6267), 1533–1537, doi:10.1126/science.aaa8026, 2015.

Robson, J., Ortega, P. and Sutton, R.: A reversal of climatic trends in the North Atlantic since 2005, Nature Geoscience, 9(7), 513–517, doi:10.1038/ngeo2727, 2016.

30 Robson, J., Polo, I., Hodson, D. L. R., Stevens, D. P. and Shaffrey, L. C.: Decadal prediction of the North Atlantic subpolar gyre in the HiGEM high-resolution climate model, Clim Dyn, 50(3), 921–937, doi:10.1007/s00382-017-3649-2, 2018.

Rödenbeck, C., Bakker, D. C. E., Gruber, N., Iida, Y., Jacobson, A. R., Jones, S., Landschützer, P., Metzl, N., Nakaoka, S., Olsen, A., Park, G.-H., Peylin, P., Rodgers, K. B., Sasse, T. P., Schuster, U., Shutler, J. D., Valsala, V., Wanninkhof, R. and Zeng, J.: Data-based estimates of the ocean carbon sink variability – first results of the Surface Ocean pCO2 Mapping intercomparison (SOCOM), Biogeosciences, 12(23), 7251– 7278, doi:https://doi.org/10.5194/bg-12-7251-2015, 2015.

Sabine, C. L., Feely, R. A., Gruber, N., Key, R. M., Lee, K., Bullister, J. L., Wanninkhof, R., Wong, C. S., Wallace, D. W. R., Tilbrook, B., Millero, F. J., Peng, T.-H., Kozyr, A., Ono, T. and Rios, A. F.: The Oceanic Sink for Anthropogenic CO2, Science, 305(5682), 367–371, doi:10.1126/science.1097403, 2004.

40 <u>Schuster, U., Watson, A. J., Bates, N. R., Corbiere, A., Gonzalez-Davila, M., Metzl, N., Pierrot, D. and Santana-Casiano, M.: Trends in North</u>
 40 <u>Atlantic sea-surface fCO2 from 1990 to 2006, Deep Sea Research Part II: Topical Studies in Oceanography, 56(8), 620–629,</u>
 <u>doi:10.1016/j.dsr2.2008.12.011, 2009.</u>

Schuster, U., McKinley, G. A., Bates, N., Chevallier, F., Doney, S. C., Fay, A. R., González-Dávila, M., Gruber, N., Jones, S., Krijnen, J., Landschützer, P., Lefèvre, N., Manizza, M., Mathis, J., Metzl, N., Olsen, A., Rios, A. F., Rödenbeck, C., Santana-Casiano, J. M., Takahashi, T., Wanninkhof, R. and Watson, A. J.: An assessment of the Atlantic and Arctic sea–air CO2 fluxes, 1990–2009, Biogeosciences, 10(1), 607–627, doi:https://doi.org/10.5194/bg-10-607-2013_2013

45 <u>doi:https://doi.org/10.5194/bg-10-607-2013, 2013.</u>

15

20

35

Signorini, S. R., Häkkinen, S., Gudmundsson, K., Olsen, A., Omar, A. M., Olafsson, J., Reverdin, G., Henson, S. A., McClain, C. R. and Worthen, D. L.: The role of phytoplankton dynamics in the seasonal and interannual variability of carbon in the subpolar North Atlantic – a modeling study, Geoscientific Model Development, 5(3), 683–707, doi:https://doi.org/10.5194/gmd-5-683-2012, 2012.

Takahashi, T., Sutherland, S. C., Wanninkhof, R., Sweeney, C., Feely, R. A., Chipman, D. W., Hales, B., Friederich, G., Chavez, F., Sabine, C.,
Watson, A., Bakker, D. C. E., Schuster, U., Metzl, N., Yoshikawa-Inoue, H., Ishii, M., Midorikawa, T., Nojiri, Y., Körtzinger, A., Steinhoff, T.,
Hoppema, M., Olafsson, J., Arnarson, T. S., Tilbrook, B., Johannessen, T., Olsen, A., Bellerby, R., Wong, C. S., Delille, B., Bates, N. R. and de
Baar, H. J. W.: Climatological mean and decadal change in surface ocean pCO2, and net sea–air CO2 flux over the global oceans, Deep Sea
Research Part II: Topical Studies in Oceanography, 56(8–10), 554–577, doi:10.1016/j.dsr2.2008.12.009, 2009.

Thierry, V., Boisséson, E. de and Mercier, H.: Interannual variability of the Subpolar Mode Water properties over the Reykjanes Ridge during 10 1990-2006, Journal of Geophysical Research: Oceans, 113(C4), doi:10.1029/2007JC004443, 2008.

Takahashi, T., Sutherland, S. C., Chipman, D. W., Goddard, J. G., Ho, C., Newberger, T., Sweeney, C. and Munro, D. R.: Climatological distributions of pH, pCO2, total CO2, alkalinity, and CaCO3 saturation in the global surface ocean, and temporal changes at selected locations, Marine Chemistry, 164, 95–125, doi:10.1016/j.marchem.2014.06.004, 2014.

Thomas, H., Prowe, A. E. F., Lima, I. D., Doney, S. C., Wanninkhof, R., Greatbatch, R. J., Schuster, U. and Corbière, A.: Changes in the North
 Atlantic Oscillation influence CO2 uptake in the North Atlantic over the past 2 decades, Global Biogeochemical Cycles, 22(4),
 doi:10.1029/2007GB003167, 2008.

Tilbrook, B., Jewett, E. B., DeGrandpre, M. D., Hernandez-Ayon, J. M., Feely, R. A., Gledhill, D. K., Hansson, L., Isensee, K., Kurz, M. L., Newton, J. A., Siedlecki, S. A., Chai, F., Dupont, S., Graco, M., Calvo, E., Greeley, D., Kapsenberg, L., Lebrec, M., Pelejero, C., Schoo, K. L. and Telszewski, M.: An Enhanced Ocean Acidification Observing Network: From People to Technology to Data Synthesis and Information Exchange, Front. Mar. Sci., 6, doi:10.3389/fmars.2019.00337, 2019.

20

Tilstone, G. H., Miller, P. I., Brewin, R. J. W. and Priede, I. G.: Enhancement of primary production in the North Atlantic outside of the spring bloom, identified by remote sensing of ocean colour and temperature, Remote Sensing of Environment, 146, 77–86, doi:10.1016/j.rse.2013.04.021, 2014.

Tjiputra, J. F., Olsen, A., Assmann, K., Pfeil, B. and Heinze, C.: A model study of the seasonal and long-term North Atlantic surface CO2 variability, Biogeosciences, 9(3), 907–923, doi:https://doi.org/10.5194/bg-9-907-2012, 2012.

Tjiputra, J. F., Olsen, A., Bopp, L., Lenton, A., Pfeil, B., Roy, T., Segschneider, J., Totterdell, I. and Heinze, C.: Long-term surface pCO2 trends from observations and models, Tellus B: Chemical and Physical Meteorology, 66(1), 23083, doi:10.3402/tellusb.v66.23083, 2014.

Touratier, F., Azouzi, L. and Goyet, C.: CFC-11, Δ 14C and 3H tracers as a means to assess anthropogenic CO2 concentrations in the ocean, Tellus B, 59(2), 318–325, doi:10.1111/j.1600-0889.2006.00247.x, 2007.

30 Ullman, D. J., McKinley, G. A., Bennington, V. and Dutkiewicz, S.: Trends in the North Atlantic carbon sink: 1992–2006, Global Biogeochemical Cycles, 23(4), doi:10.1029/2008GB003383, 2009.

Uppström, L. R.: The boron/chlorinity ratio of deep-sea water from the Pacific Ocean, Deep Sea Research and Oceanographic Abstracts, 21, 161–162, doi:10.1016/0011-7471(74)90074-6, 1974.

Våge, K., Pickart, R. S., Moore, G. W. K. and Ribergaard, M. H.: Winter Mixed Layer Development in the Central Irminger Sea: The Effect of
 Strong, Intermittent Wind Events, J. Phys. Oceanogr., 38(3), 541–565, doi:10.1175/2007JPO3678.1, 2008.

Vázquez-Rodríguez, M., Pérez, F. F., Velo, A., Ríos, A. F. and Mercier, H.: Observed acidification trends in North Atlantic water masses, Biogeosceinces, 9, 5217-5230, doi: https://doi.org/10.5194/bg-9-5217-2012, 2012.

Wakita, M., Watanabe, S., Honda, M., Nagano, A., Kimoto, K., Matsumoto, K., Kitamura, M., Sasaki, K., Kawakami, H., Fujiki, T., Sasaoka, K., Nakano, Y. and Murata, A.: Ocean acidification from 1997 to 2011 in the subarctic western North Pacific Ocean, Biogeosciences, 10(12), 7817–7827, doi:https://doi.org/10.5194/bg-10-7817-2013, 2013.

Wakita, M., Nagano, A., Fujiki, T. and Watanabe, S.: Slow acidification of the winter mixed layer in the subarctic western North Pacific, Journal of Geophysical Research: Oceans, 122(8), 6923–6935, doi:10.1002/2017JC013002, 2017.

Wanninkhof, R., Pickers, P. A., Omar, A. M., Sutton, A., Murata, A., Olsen, A., Stephens, B. B., Tilbrook, B., Munro, D., Pierrot, D., Rehder, G., Santana-Casiano, J. M., Müller, J. D., Trinanes, J., Tedesco, K., O'Brien, K., Currie, K., Barbero, L., Telszewski, M., Hoppema, M., Ishii, M., González-Dávila, M., Bates, N. R., Metzl, N., Suntharalingam, P., Feely, R. A., Nakaoka, S., Lauvset, S. K., Takahashi, T., Steinhoff, T.

and Schuster, U.: A Surface Ocean CO2 Reference Network, SOCONET and Associated Marine Boundary Layer CO2 Measurements, Front. Mar. Sci., 6, doi:10.3389/fmars.2019.00400, 2019.

Watson, A. J., Schuster, U., Bakker, D. C. E., Bates, N. R., Corbière, A., González-Dávila, M., Friedrich, T., Hauck, J., Heinze, C., Johannessen, T., Körtzinger, A., Metzl, N., Olafsson, J., Olsen, A., Oschlies, A., Padin, X. A., Pfeil, B., Santana-Casiano, J. M., Steinhoff, T., Telszewski, M., Rios, A. F., Wallace, D. W. R. and Wanninkhof, R.: Tracking the Variable North Atlantic Sink for Atmospheric CO2, Science, 326(5958), 1391–1393, doi:10.1126/science.1177394, 2009.

5

Weiss, R. F. and Price, B. A.: Nitrous oxide solubility in water and seawater, Marine Chemistry, 8(4), 347-359, doi:10.1016/0304-4203(80)90024-9, 1980.

Williams, N. L., Juranek, L. W., Feely, R. A., Johnson, K. S., Sarmiento, J. L., Talley, L. D., Dickson, A. G., Gray, A. R., Wanninkhof, R.,
 Russell, J. L., Riser, S. C. and Takeshita, Y.: Calculating surface ocean pCO2 from biogeochemical Argo floats equipped with pH: An uncertainty analysis, Global Biogeochemical Cycles, 31(3), 591–604, doi:10.1002/2016GB005541, 2017.